Antimalarials in Development in 2014

ARTICLE *in* CHEMICAL REVIEWS · OCTOBER 2014

Impact Factor: 46.57 · DOI: 10.1021/cr500543f · Source: PubMed

2 AUTHORS:

David Barnett
St. Jude Children's Research Hospital
5 PUBLICATIONS **96** CITATIONS
SEE PROFILE

Kip Guy
St. Jude Children's Research Hospital
186 PUBLICATIONS **7,111** CITATIONS
SEE PROFILE

CHEMICAL REVIEWS

Review

pubs.acs.org/CR

Antimalarials in Development in 2014

David S. Barnett and R. Kiplin Guy*

Department of Chemical Biology and Therapeutics, St. Jude Children's Research Hospital, Memphis, Tennessee 38105, United States

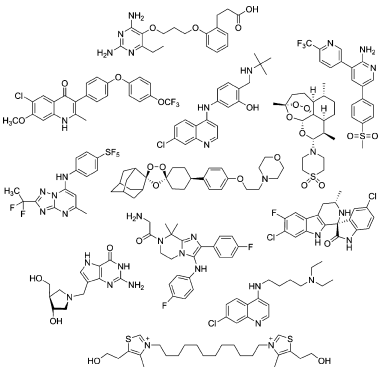

CONTENTS

1. INTRODUCTION

Malaria continues to be a devastating burden on the world, causing the deaths of an estimated 627 000 people in 2012, with 482 000 of those being children under the age of 5.[1] The emergence of resistance to the current frontline antimalarial artemisinins[2] drives the need for the continued development of new drugs targeting novel therapeutic pathways. In the past few decades, a number of programs focusing on the rational design of antimalarials have delivered the culmination of their efforts by delivering compounds into the clinic. In the same time frame, the paradigm for early antimalarial drug discovery has shifted with the development of high-throughput phenotypic screening as a strategy for unbiased early lead discovery. These programs are also delivering compounds into the clinic.

The hallmarks of an ideal antimalarial drug, which have recently been reviewed,[3] include potent activity against *Plasmodium* species causing human pathogenesis (especially *Plasmodium falciparum* and *Plasmodium vivax*), oral bioavailability, rapid speed of action, a very strong safety profile, and a low cost of treatment to provide access to the populations hardest hit by the disease. It is also highly desirable for antimalarials to display exoerythrocytic activity, which includes activity toward the sexual (gametocyte) and liver (especially hypnozoite) stages of the parasite life cycle to provide transmission-blocking and prophylactic activity, respectively. Following our previous review of known antimalarials[4] and other antimalarial reviews,[5] in this review we seek to outline chemotypes currently in clinical development for the treatment of malaria.

2. IDENTIFICATION OF ANTIMALARIALS BY RATIONAL DESIGN

2.1. 4-Aminoquinolines

Aminoquinolines have been a backbone of antimalarial drugs since the 1940s. Since the emergence of resistance to chloroquine (CQ)[6] arising from multiple mutations in the *Pf*CRT gene, efforts have focused on identifying new aminoquinoline analogues that do not share cross-resistance with CQ. These efforts led to the identification of analogues currently in development, including 4-aminoquinoline ferroquine[7] and the 8-aminoquinolines tafenoquine and NPC-1161B[8] (Figure 1).

In the middle 1990s, an effort to revive CQ through modification of the aminoquinoline side chain led to the

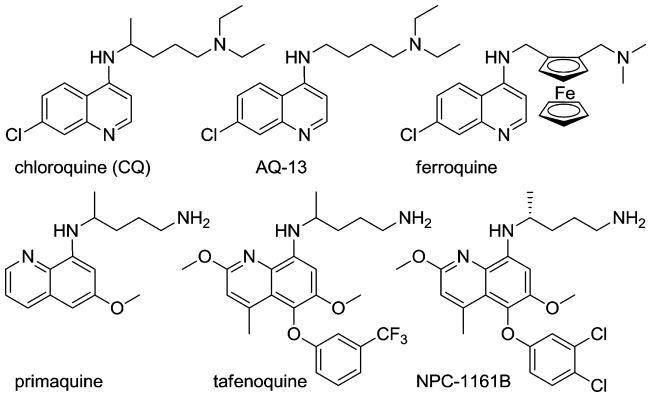

Figure 1. Other 4-aminoquinoline and 8-aminoquinoline analogues.

Special Issue: 2014 Drug Discovery and Development for Neglected Diseases

Received: September 25, 2014
Published: October 23, 2014

   dx.doi.org/10.1021/cr500543f | *Chem. Rev.* 2014, 114, 11221−11241

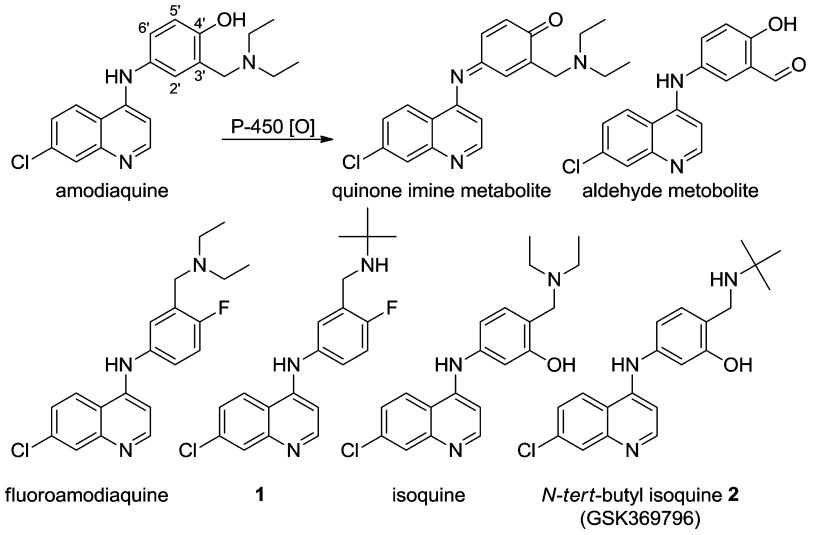

Figure 2. Development of isoquine and analogues.

rediscovery of AQ-13,[9] a CQ analogue originally discovered in the late 1940s that had previously exhibited activity against *P. vivax* in vivo.[10] The study demonstrated that the branched isopentyl side chain of CQ could be replaced with unbranched ethyl, propyl, isopropyl, decyl, or dodecyl side chains (AQ-2l, AQ-13, AQ-34, AQ-41, or AQ-40), with the new analogues being active against CQ-resistant strains of *P. falciparum* in vitro.[9] AQ-13 was chosen as the preclinical candidate on the basis of enhanced in vivo potency displayed in monkey models (*P. vivax* and CQ-resistant *P. falciparum*) in addition to cost considerations.[11] When assessed in animal models, AQ-13 possessed a toxicology[12] and pharmacokinetic profiles[13] comparable to those of CQ. A phase I trial of AQ-13 revealed a tolerability profile in humans similar to that of CQ (headache, lightheadedness, and gastrointestinal (GI) tract adverse events (AEs) most common), with demonstrated safe doses of up to 1750 mg.[11] The pharmacokinetics were similar to those of CQ, although there was lower apparent exposure of AQ-13 due to more rapid clearance, requiring higher doses to achieve equivalent exposures. AQ-13 is currently undergoing a phase II trial with subjects with uncomplicated malaria (ClinicalTrials.gov identifier NCT01614964).

The 4-aminoquinoline amodiaquine (Figure 2) is an analogue of CQ[14] that has shown efficacy against CQ-resistant isolates.[15] However, clinical use has been limited due its association with hepatotoxicity and agranulocytosis.[16] In vivo studies have shown that, upon administration of amodiaquine to rats, the compound is excreted in the bile exclusively as 5′-thioether conjugates (glutathione and cysteinyl),[17] which indicates that metabolism occurs through the formation of amodiaquine quinonimine or semiquinonimine (Figure 2) that is subsequently glutathionylated.[18] In addition, an aldehyde metabolite was identified following incubation of amodiaquine with human liver microsomes from the phase I metabolism of the Mannich base side chain.[19] These biotransformations are believed to cause the clinically observed toxicities through bioconjugation of the resultant metabolites. The elucidation of these metabolic transformations[19,20] led to a campaign to identify a metabolically stable analogue of amodiaquine.

A rational design approach switching the positions of the 4′-phenol and the 3′-Mannich base side chain provided isoquine (Figure 2), a regioisomer of amodiaquine incapable of forming the reactive intermediate.[21] The synthesis of isoquine was achieved through a cost-effective, two-step route from commercially available starting materials utilizing a Mannich reaction to furnish the requisite side chain. Both isoquine and its diphosphate salt were highly potent in vitro (EC_{50} < 20 nM) against *P. falciparum* and in vivo against *Plasmodium yoelii* NS infected mice (ED_{50} = 3 mg/kg, po (per os)). The diphosphate salt was almost 3-fold more potent than amodiaquine, and evaluation of the pharmacokinetics (PK) of isoquine in vivo showed a 3-fold increase in plasma levels compared to those for amodiaquine. No conjugates were found with isoquine, which suggested the compound was not bioactivated. The major metabolites identified for isoquine were glucuronides, which were not observed for amodiaquine or its metabolites. However, the observation of high first-pass metabolism of the *N*-diethylamino Mannich side chain compelled further efforts to identify analogues with clinically acceptable PK profiles.

Prior to the identification of isoquine, metabolic stability studies with amodiaquine determined that, like paracetamol (acetaminophen),[22] the replacement of the phenol substituent with a fluorine atom to produce fluoroamodiaquine (Figure 2) provided superior metabolic stability.[23] Although the in vitro antiplasmodial potency of the metabolically stable fluorinated analogues was 2-fold lower than that of amodiaquine, the in vivo potency of fluoroamodiaquine against *Plasmodium berghei* infected mice was equivalent. Cost considerations initially limited development of fluoroamodiaquine until an improved synthetic route reinvigorated the program.[24] From the series of new analogues synthesized, *tert*-butyl analogue **1** (Figure 2) displayed the highest in vitro potency against both CQ-sensitive and CQ-resistant parasites, equivalent to that of CQ and isoquine, although it was not quite as potent as amodiaquine. Analysis of in vivo activity against *P. berghei* ANKA infected CD1 mice in the standard four-day test[25] determined an ED_{50} value for **1** of 5 mg/kg. Compound **1** was efficacious against *P. yoelii*, with an ED_{50} value of 8 mg/kg, although recrudescence was observed for **1** and the control compounds CQ and amodiaquine at the highest dose (40 mg/kg).

Pharmacokinetic studies using ^{3}H-labeled **1** in rat showed significantly lower accumulation in the brain, kidneys, liver, and skin compared to that of amodiaquine 5 h following the administration of equivalent doses.[24] **1** was largely eliminated

by 24 h postdose, with the majority of compound found unchanged in the urine, and completely cleared after 10 days. Overall, **1** showed a pattern of distribution similar to that of 4-aminoquinolines, with the highest levels being found in the liver and skin. Metabolite analysis following administration of [^{3}H]**1** to male Wistar rats (54 μmol/kg, 20 μCi) found nine metabolites with no evidence of P450 hydroxylation of the 4′-fluoro aromatic ring, indicating the elimination of the formation of toxic metabolites for the fluorinated analogue. Comparison of the PK parameters of **1** with those of amodiaquine showed superior bioavailability of 100% in rat and 37% in mouse for **1** compared to a mean oral bioavailability of less than 20% for amodiaquine. Exposure in the mouse was comparable to that of CQ after administration of a single 10 mg/kg dose with equivalent areas under the curve (AUCs) over 24 h and similar elimination half-lives (∼7 h in noninfected mice). Whole blood concentrations were also significantly higher in infected animals compared to noninfected animals, which was attributed to selective accumulation into parasitized red blood cells (RBCs). As expected, intrinsic clearance of **1** was lower in hepatocytes from human and four animal species compared to that of both amodiaquine and isoquine. Fluoro analogue **1** was also found to inhibit CYP 2D6.[26] Safety profiles were also favorable, showing a large therapeutic index in vitro, no mutagenicity, and an in vivo maximal nonlethal dose (MNLD) (610 mg/kg, po dose) and a no observed adverse effect level (NOAEL) (300 mg/kg single dose) similar to those of CQ and amodiaquine.[24] Further work has not been reported.

The metabolism advantages gained from the introduction of the *N*-*tert*-butyl moiety in **1** suggested that incorporation of this substitution into isoquine would provide a simplified metabolic profile and enhanced oral bioavailability.[27] *N*-*tert*-Butylisoquine (**2**, Figure 2) was synthesized and evaluated against a variety of *P. falciparum* isolates in vitro, where it displayed potent activity against both CQ-resistant (K1 EC_{50} = 13 nM) and CQ-sensitive (EC_{50} = 11 and 13 nM for 3D7 and HB3, respectively) parasites. The oral potency in vivo (ED_{50} = 2.8 mg/kg against *P. berghei* ANKA infected mice) was equivalent to that of amodiaquine, but the better exposure profile led to the prevention of recrudescence with a 20 mg/kg dose, whereas CQ, amodiaquine, and analogue **1** all failed to prevent recrudescence at doses up to 40 mg/kg. Field reports of the failure of amodiaquine[28] initially sparked concern over developing analogues, but subsequent culture of both parasites collected predose and following recrudescence showed that **2** displayed activity superior to that of both CQ and the active metabolite of amodiaquine, desethylamodiaquine, in vitro.[27] In a drive to reduce cost and scale up the synthesis of **2**, the order of the two-step reaction was reversed and the Mannich reaction optimized to provide **2** in 59% yield and >98% purity on a multikilogram scale,[29] thereby satisfying the target product profile (TPP) criteria for an affordable antimalarial.

Detoxification of heme that is generated from the degradation of hemoglobin by the parasite through the crystallization of heme into hemozoin is required for the survival of the parasite, and the prevention of hemazoin formation by binding to heme has been established as the mechanism of action for CQ.[30] Mechanistic studies were conducted using a UV−vis spectroscopic method to accurately determine binding constants through titrations of compound into monomeric heme species in solution,[31] and from the observation of similar equilibrium binding constants of **1** and **2** to both CQ and amodiaquine, a common mechanism of action is suggested.[27] Subsequent molecular modeling of the interaction of **2** with the drug target hematin[32] showed that the most favorable complex is consistent with a $\pi-\pi$ stacking interaction[14] and a favorable hydrogen-bonding network between the carboxylate groups of hematin and the alcohol and protonated amine of the Mannich side chain.[27]

Analysis of PK profiles in mouse, rat, dog, and/or monkey comparing **2** with isoquine and desethylisoquine[33] demonstrated that the blood clearance of **2** was the lowest and its bioavailability was higher (≥68%) than that of isoquine (≤21%). The steady-state distribution volume was high for **2**, exceeding total body water in all species, and the elimination half-lives were moderate (3 h in mouse and 11 h in monkey). Like **1**, substantial partitioning into RBCs was observed. Metabolism studies of **2** following incubation in hepatocytes from mouse, rat, dog, and human showed no evidence of glutathione conjugation or reactive metabolite formation despite the observation of multiple metabolites, confirming the metabolic advantage of the *tert*-butylamine substitution. The metabolites observed in vitro were consistent with the urinary and biliary metabolites observed following the administration of [^{3}H]isoquine to rats.

Toxicological profiling of **2** revealed no genotoxicity in vitro in a bacterial mutation assay and mouse lymphoma assay or in an in vivo mouse micronucleus assay.[27] The potential for adverse central nervous system (CNS) activity was similar to that of CQ and amodiaquine with evident antagonistic activity of muscarinic and 5HT receptors and adverse dose-related CNS effects (respiratory depression, tremors, and convulsions). Dose range finding studies in mouse, rat, dog, and nonhuman primate found evidence of changes related to phospholipidosis which did not affect normal organ function, were generally reversible, and were seen at exposures comparable to those predicted for human efficacy. Toxicology studies in rats over 4−14 day durations showed cardiovascular toxicity, principally myocardial necrosis, skeletal muscle myopathy, and hepatic effects (hypertrophy, transaminase release, and apoptosis) in addition to CNS effects. Repeat dose toxicity studies in monkeys showed dose-limiting CNS effects at plasma drug levels approximately 3-fold higher than the clinical target, while lower doses revealed minor hepatocellular hypertrophy, serum transaminase increases (up to 5-fold), and phospholipidosis in multiple tissues. Inhibition of the human ether-a-go-go related gene (hERG) potassium ion channel repolarization was also observed at levels comparable to those of other antimalarials, and mild, transient increases in corrected QT interval (QTc) were observed in monkeys along with some electrocardiogram (ECG) rhythm abnormalities,[27] similar to cardiac effects reported in man following CQ administration.[34] Generally, the toxicology seen with **2** was similar to that seen with CQ, amodiaquine, and piperaquine. While adverse toxicology was observed in these studies, four sequential daily doses in rats at tolerated doses did not induce the cardiac effects that are apparent with similar dosing of CQ, suggesting it will have a better cardiac safety profile. *N*-*tert*-Butylisoquine (GSK369796) has completed phase I clinical trials to assess the safety of single ascending doses in healthy volunteers (ClinicalTrials.gov identifier NCT00675064).

2.2. Endoperoxides

Since the discovery of the antimalarial activity of artemisinin (ART) in China in the late 1960s, ART and its derivatives have emerged as the frontline drugs for the treatment of malaria.

ART is a complex sesquiterpene lactone natural product that is most practically obtained by isolation from its natural source, *Artemisia annua* L.[35] ART can also be manufactured through partial synthesis from the more abundant intermediate, artemisinic acid. Recently, a fermentation process to produce artemisinic acid from simple, inexpensive carbon substrates with genetically engineered *Saccharomyces cerevisiae* has been reported.[36] In addition, dihydroartemisinic acid can be converted directly to ART via a continuous flow sequence that is initiated with a photochemically induced oxidation by singlet oxygen followed by an acid-mediated cleavage of the oxygen−oxygen bond (Hock cleavage) with a final oxidation step by triplet oxygen, providing an intermediate that subsequently rearranges to provide ART in 69% yield.[37] This flow methodology has recently been extended to the production of artesunate (ATS) (3.4 mmol/h, 28% yield) with the implementation and optimization of $NaBH_4$-packed columns to achieve efficient reduction of ART to dihydroartemisinin (DHA).[38] Total syntheses of ART have been accomplished, but the routes are too cost prohibitive to be implemented in the production of antimalarial therapeutics.[39] Although ART derivatives show rapid onset of action and potent activity against all erythrocytic stages of the parasite, they display short in vivo half-lives and low bioavailability.[40] Strategies to improve the performance of endoperoxide antimalarials include chemical modifications of ART to achieve more favorable pharmacokinetics and the development of completely novel trioxolane and tetraoxane scaffolds as synthetic surrogates for ART.

Efforts to improve ART focused on improving both metabolic stability and aqueous solubility while reducing lipophilicity to help facilitate bioavailability and attenuate neurotoxicity.[41] Although not seen in the clinic at efficacious doses, neurotoxicity has been observed in preclinical studies, both in vitro studies in neuronal cell cultures[42] and in vivo studies in animal models, and must be considered when developing new ART derivatives.[43] The severity of neurotoxicity has been correlated with lipophilicity.[44] In one strategy, replacing the C-10 carbonyl with various amines improved aqueous solubility and prevented the formation of DHA, the major metabolite of currently approved ART derivatives.[41] Derivatives were synthesized from DHA by converting the alcohol in the 10-position to the corresponding bromide in situ and subsequently displacing the bromide with amine nucleophiles to provide isomerically pure compounds. Artemisone (Figure 3) displayed acceptable solubility (220 μM) and showed no signs of neurotoxicity in a primary neuronal stem cell model[45] (IC_{50} values for artemisone of >25000 nM compared to an IC_{50} value of 35 nM for DHA). Artemisone also showed no effect on intracellular ATP levels in mammalian cells, a metric used to measure mitochondrial health,[46] at the highest concentration tested (IC_{50} for artemisone of >25000 nM compared to IC_{50} = 280 nM for DHA).[41] While artemisone was not the most potent ART derivative synthesized, it showed the most favorable toxicity profile and physiochemical properties and was therefore selected as the development candidate.

In comparative in vitro screens against a panel of sensitive and multi-drug-resistant strains of *P. falciparum* (3D7, K1, VS1, 7G8, HB3-B2, FCB, FCR3, Tm90 C2A, W2, FCR-8, FCC2, and DD2), artemisone was found to be substantially more potent (IC_{50} values of <2.5 nM) than CQ, pyrimethamine (PYR), and ATS.[41] Artemisone was efficacious in vivo (ED_{90} = 3.1 mg/kg (po) and 1.5 mg/kg (sc, subcutaneously)) against the CQ-sensitive *P. berghei* N strain and the CQ-resistant *P. yoelii* NS strain (ED_{90} = 5.0 mg/kg (po) and 3.9 mg/kg (sc)). Subsequent studies demonstrated efficacy in vivo in *Aotus* monkeys infected with *P. falciparum* FVO isolates (resistant to CQ and antifolates) at 10 mg/kg/day (po) over 3 days. Artemisone cleared all parasites in each monkey (n = 4) within 24 h following treatment, while parasites were still observed 48 h after completion of treatment in monkeys treated with ATS. In this study, one of three monkeys was cured by artemisone, whereas recrudescence occurred for all monkeys given ATS. Artemisone (10 mg/kg) was fully curative when given in combination with mefloquine (MFQ; 5 mg/kg) or amodiaquine (AQ; 20 mg/kg). While the mechanism of action of ART has not been unequivocally determined, inhibition of the putative target, parasite Ca^{2+} pump *Pf*ATP6,[47] was found to be more potent for artemisone than ART (K_i values for ART and artemisone against *P. falciparum* are 169 ± 31 and 1.7 ± 0.6 nM, respectively, and those against the *P. vivax* orthologue are 8 ± 5 and 0.07 ± 0.01 nM, respectively[48]).

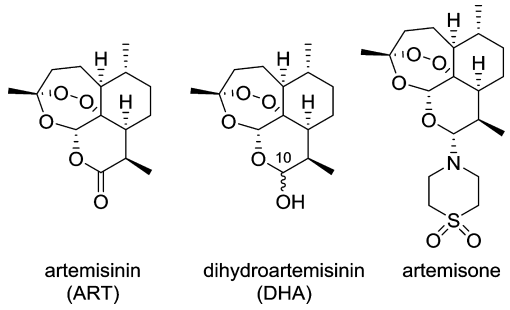

Figure 3. Development of artimisone.

Phase I trials with healthy male volunteers established the safety, tolerability, and pharmacokinetics of artemisone.[49] Daily doses over 3 days of 40 and 80 mg were well tolerated and caused no serious adverse events except for elevations in liver function tests observed for a single patient in the study. The oral pharmacokinetics of artemisone are characterized by rapid absorption (T_{max} ≈ 1.5 h), moderate clearance (237 L/h), a moderately high apparent volume of distribution (13.7 L/kg), and a relatively rapid elimination half-life (3.1 h) following the last dose of the 3 day course of 80 mg. Dose-proportional increases in the AUC were observed for five escalating single doses. To identify metabolites, radiolabeled artemisone was incubated with liver microsomes and hepatocytes sourced from humans, dogs, and rats, revealing three major metabolites but no observable formation of DHA, the major neurotoxic metabolite of ART derivatives.[41] The three major metabolites identified in vitro were also formed rapidly and extensively in vivo and determined to have antimalarial activity,[50] albeit with a reduced potency compared to that of the parent artemisone.[49] Artemisone is currently awaiting phase II interventional studies for the treatment of uncomplicated *P. falciparum* malaria.

In addition to derivatization of ART, the exploration of novel, synthetic endoperoxides has helped facilitate access and improve pharmacological properties of endoperoxide antimalarials. Numerous early attempts to pursue peroxide-containing compounds as alternatives to ART yielded little success.[51] However, significant progress has been reported for the development of completely synthetic antimalarial endoperoxides. An initial effort focused on 1,2,4-trioxolanes that were synthesized and assayed for antimalarial activity.[52] Synthesis of

1,2,4-trioxolane analogues was accomplished through a Griesbaum co-ozonolysis[53] coupling of symmetrical *O*-methyl 2-adamantanone oxime with cyclohexanones. X-ray structural analysis of a selected chiral analogue determined the relationship between the peroxide group and the substituent on the cyclohexane ring to be *cis*. Both the symmetric dicyclohexyl and diadamantyl analogues (**3** and **4**, Figure 4) were found to be inactive, whereas the mixed cyclohexyl- and adamantyl-substituted trioxolane and the cyclohexanone variant (**5** and **6**, Figure 4) displayed good potency against *P. falciparum* in vitro and efficacy against *P. berghei* in vivo, with the potency

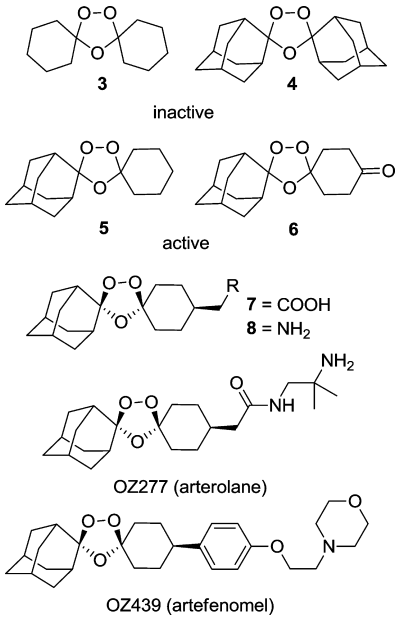

Figure 4. Development of OZ439.

being comparable to that of artesunate. This study provided the key structure−activity relationship insight that the major driver for potency was the steric accessibility of the peroxide bond, with maximum potency being achieved with sterics that were neither too exposed nor too hindered. The peroxide bond itself was also determined to be essential for activity.[54] These active compounds, and a closely related analogue set,[55] were very lipophilic and displayed poor aqueous solubility and low bioavailability in rats. Therefore, the identification of analogues with enhanced solubility became the primary focus of the program.

A significant advance was achieved when the carboxylic acid-substituted analogue (**7**, Figure 4) was found to exhibit high oral bioavailability (74%) and a moderate (2 h) half-life after oral administration of a 50 mg/kg dose to rats.[52] This represented a substantial improvement over artesunate, albeit with lower potency (IC_{50} = 106 nM compared to 4 nM for artesunate). Exchange of the carboxylic acid for an amine (**8**) significantly increased potency (IC_{50} = 1 nM) while maintaining reasonable bioavailability (30%); this compound cured *P. berghei* infected mice[25] with 3 × 10 mg/kg daily oral doses. These early successes led to a full lead optimization campaign[56] ultimately identifying the clinical candidate OZ277 (Figure 4). Like the ART derivatives, OZ277 exhibited a rapid onset of action in vivo while maintaining activity against all asexual blood stages of the parasite.[57] The pharmacokinetic behavior was substantially improved with both **8** and OZ277 having superior half-lives compared to dihydroartemisinin (DHA)[40b] following intravenous injection and oral bioavailability greatly exceeding that of artemether and comparable to that of artesunate.[52] During development it was discovered that compound blood concentrations were 2.5 times higher in uninfected mice compared to compound plasma concentrations. Subsequent studies suggest a further partitioning of OZ277 in infected RBCs over uninfected RBCs.[58] This phenomenon causes an underestimate of the compound concentration at the site of action when analyzing plasma drug concentrations.[59] Following oral administration, compound **8** was distributed in significant concentrations to the liver, kidney, brain, lung, and heart, whereas tissue concentrations for OZ277 were 2−5-fold lower with no measurable concentration observed in brain tissue, suggesting a lower risk of neurotoxicity for OZ277.[60]

While the in vitro potencies of both **8** and OZ277 against *P. falciparum* strains K1 and NF54 were on par with those of artesunate and artemether, the in vivo potency was superior.[52] Analogue **8** cured all infected mice in the *P. berghei* in vivo model without recrudescence and in combination with chloroquine provided complete protection when administered 24 h prior to infection. In contrast, recrudescence was observed for OZ277 with no prophylaxis being observed. While analogue **8** displayed better pharmacokinetics and more favorable pharmacodynamics, OZ277 was ultimately chosen as a clinical candidate due to a more favorable toxicological profile. OZ277 was ultimately carried through phase IIa studies in a collaboration between the Medicines for Malaria Venture (MMV) and the Indian company Ranbaxy, which named the compound Rbx11160.[61] These trials showed 3-fold lower exposures for infected patients compared with those displayed in healthy individuals with day 28 cure rates of only 60−70%. In addition, OZ277 gave increased AUC values in patients when the parasite burden was reduced.[62] The compound was withdrawn from development by MMV, although Ranbaxy has pursued the compound independently and has introduced the combination with piperaquine in India as the drug Synriam.[63]

Efforts to improve the pharmacokinetic properties of the series focused on identifying the mechanism of clearance leading to the suboptimal half-life of OZ277. Metabolism studies revealed that cytochrome P450 (CYP450) mediated oxidation produced several inactive hydroxylated adamantane metabolites.[64] Although predosing rats with the irreversible CYP450 inhibitor 1-aminobenzotriazole reduced the clearance from 61 to 31 mL/min/kg,[65] the effect was lower than would be expected if CYP450 were the only contributing factor to drug clearance.[66] Further mechanistic studies suggested that reductive activation of the peroxide bond by Fe(II) or liberated heme was critical to activity and contributed to clearance.[67] Further studies suggested that endogenous sources of Fe(II) in blood and tissues were likely causing the rapid drug clearance.[65] In addition, OZ277 was found to be 5-fold less stable in human blood containing low levels of parasitemia (1% at 45% hematocrit) compared to that in uninfected blood. These data suggested that the lower observed exposure of OZ277 in malaria patients was due to the increased rate of degradation in the presence of parasites. Studying the degradation kinetics of 1,2,4-trioxolane analogues in the presence of $FeSO_4$ revealed that increasing the steric bulk on the cyclohexane substituent leads to greater stability to iron degradation,[68] which was supported by computational analysis which showed that the more stable analogues can adopt conformations that sterically

shield the peroxide bond.[69] These findings led to the replacement of the *cis*-8′-alkyl substituent of OZ277 with a phenyl ring, thus providing a >50-fold increase in stability toward Fe(II)-mediated degradation. This led to the discovery of OZ439 (Figure 4).[65] Evaluation of the stability of OZ439 revealed a 15-fold increase in stability in healthy rat blood and a 20-fold increase in stability in healthy human blood compared to that of OZ277.

The enhanced in vitro blood stability of OZ439 suggested more favorable pharmacokinetics were likely.[65] Indeed, the resulting AUC for OZ439 from a 3 mg/kg oral dose in rats was found to be 10-fold greater than that for OZ277 with improvements in bioavailability, increased volume of distribution, and an extended half-life (>20 h). This performance represents a substantial improvement relative to that of either DHA (∼0.5 h) or OZ277 (1 h). Plasma concentration versus time profiles for OZ439 were also found to increase proportionally across the dose range of 3−30 mg/kg. In vitro antiplasmodial potency for OZ439 ranged from 0.9 to 7 nM, which is comparable to that of other synthetic peroxides and ART derivatives. Activity was maintained across all asexual blood stages with IC_{50} values of 4, 6, and 6 nM for rings, trophozoites, and schizonts, respectively. The in vivo potency for OZ439 in the *P. berghei* mouse model was excellent, with a single oral dose of 20 mg/kg or three daily doses of 5 mg/kg being completely curative. OZ439 also had prophylactic activity, with a single oral dose of 30 mg/kg administered 48 h prior to parasite inoculation being completely protective against infection.

Phase I clinical trials showed OZ439 to be safe and well-tolerated at doses up to 1600 mg, with observed adverse events including diarrhea, nausea, and gastrointestinal hypermotility at the highest dose studied.[70] The oral pharmacokinetic profile of OZ439 in humans was good, with the maximum concentration (t_{max}) being reached after 3 h and a terminal half-life of 25−30 h. However, OZ439 concentrations were increased by 3−4.5-fold when administered with food. Plasma concentrations were maintained above 18 nM for 96 h following administration of an 800 mg oral dispersion, which satisfies the targeted exposure on the basis of preclinical pharmacodynamic models. The metabolites of OZ439 were similar to those of OZ277, and analysis of these metabolites suggested that the parent compound was solely responsible for antimalarial activity. OZ439 has completed phase IIa trials for acute uncomplicated malaria in patients with *P. falciparum* or *P. vivax* malaria monoinfection (ClinicalTrials.gov identifier NCT01213966) and is currently being evaluated in a phase IIb study to determine the efficacy of a single dose (800 mg) in combination with piperaquine (ClinicalTrials.gov identifier NCT02083380).

In a parallel effort fueled by the observation of the low in vivo stability of OZ277,[71] the closely related 1,2,4,5-tetraoxanes were developed as an alternative.[72] The driving factor for this project came from the comparison of simple dispiro-1,2,4-trioxolane **3** with the corresponding 1,2,4,5-tetraoxane **9** (Figure 5), which revealed that while the trioxolane was unstable and inactive, the tetraoxane showed good stability and potent antiplasmodial activity (IC_{50} = 25 nM).[73] Taking into account the functionality incorporated during the development of OZ277,[52] a number of tetraoxane analogues were synthesized incorporating the spiroadamantyl group to provide two series of novel tetraoxane antimalarials.[74] The focus of the synthetic efforts was to identify a metabolically stable polar side

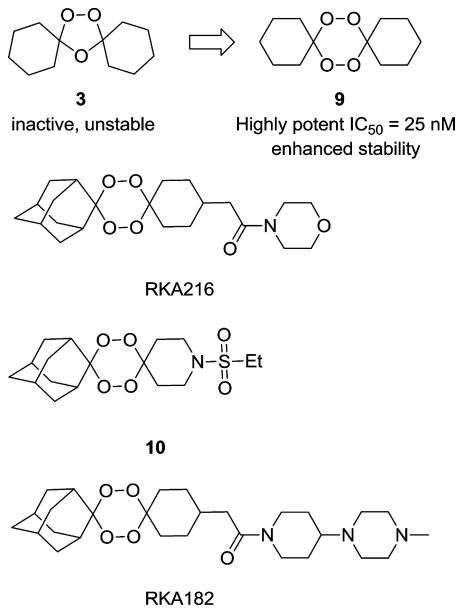

Figure 5. Development of RKA182.

chain to counterbalance the lipophilicity of the adamantyl side chain. Analogue RKA216 (Figure 5), identified from the first round of synthesis, showed potent in vitro activity (IC_{50} = 5 nM, *P. falciparum* strain 3D7) and was completely suppressive at an oral dose of 30 mg/kg in Peter's test (ED_{50} = 3 mg/kg) against *P. berghei* ANKA.[74a] The relatively lengthy six-step synthetic route to RKA216 prompted the investigation of a second series of tetraoxane analogues that could be produced using a two-step synthesis.[74b] Most of the synthesized analogues showed high potency (IC_{50} values between 3 and 30 nM), and the presence of an adamantyl group was found to greatly increase activity. Analogue **10** (Figure 5) demonstrated in vivo efficacy in *P. berghei* ANKA infected mice[75] (ED_{50} = 7 mg/kg).

Comparison of the in vitro and in vivo metabolism and pharmacokinetics of the two tetraoxane series led to the selection of RKA216 analogues over analogues of **10**, partially due to the poor bioavailability of analogues of **10**.[72] Ultimately, the synthesis and evaluation of 150 analogues led to the selection of RKA182 (Figure 5) as the development candidate. Piperidinylpiperazine-functionalized tetraoxane RKA182 displayed excellent in vitro potency against *P. falciparum* strain 3D7 (IC_{50} = 4.9 nM), as well as excellent in vivo activity (ED_{50}/ED_{90} = 2/8 mg/kg, po), prolonging mouse survival to 22 days when dosed at 3 × 10 mg/kg/day. Evaluation of the pharmacokinetics following intravenous (1 mg/kg) and oral (10 mg/kg) administration in rats revealed an oral bioavailability of 24% with equivalent exposure in both infected and noninfected mice. Formulation optimization of RKA182 led to selection of the ditosylate salt, which provided improved oral bioavailability of 38% in the rat (42% in the mouse) in addition to improved potency (ED_{50} and ED_{90} values of 1 and 4 mg/kg, respectively). RKA182 was also tested against isolates from patients who had failed ACT combination chemotherapy, where it displayed a 5−10-fold increase in potency over ART, with all IC_{50} values below 5 nM. RKA182 was fast acting as well, with parasitemia rapidly decreased to undetectable levels 24 h after treatment. While RKA182 provides a potent alternative to ART with superior stability compared to

dx.doi.org/10.1021/cr500543f | *Chem. Rev.* 2014, 114, 11221−11241

OZ277, development has been put on hold to investigate analogues with improved pharmacokinetic properties.

2.3. Phosphatidylcholine Inhibitor SAR97275

The biogenesis of phospholipid (PL) cell membranes is an essential function of the replicating malaria parasite, and the majority of PLs are phosphatidylcholine (PC) produced by the parasites from choline and fatty acids both salvaged from the host plasma.[76] Transport of choline into the infected erythrocyte is the limiting step of PC formation.[77] Treatment with quaternary ammonium choline analogues results in parasite growth inhibition.[78]

In studies aimed at developing therapeutic leads from this observation, a set of 80 analogues were assayed for antiplasmodial activity, revealing that growth inhibitory potency closely correlated to the inhibition of PC biosynthesis.[79] Structure–activity relationships (SARs) for these analogues revealed that the most potent compounds contained either one quaternary ammonium head attached to a hydrophobic chain or two quaternary ammonium groups connected by a hydrophobic chain (Figure 6).[80] Comparing antiplasmodial potency between the bisquaternary ammonium analogue G4 and the corresponding monoquaternary analogue E6 revealed a 5.5-fold increase in potency for the dication (*P. falciparum* IC_{50} = 90 and 500 nM, respectively). Systematic variation of the length of the hydrophobic linker revealed that potency increased with increasing chain length. Increasing the linker length from 12 carbons (G4) to 16 carbons (G5) provided a 20-fold increase in potency (IC_{50} = 4 nM).[81] On the other hand, by increasing the hydrophobicity and bulk enveloping the monoammonium polar head by altering the *N*-methyl substitutions to either ethyl or propyl groups, a significant reduction in potency (IC_{50} = 500 nM compared to 64 and 33 nM, respectively) was observed.[80] Systematic substitution of the alkyl groups attached to the nitrogen revealed a correlation between the hydrophobic volume surrounding the polar and the antiplasmodial potency, with the optimal volume for antiplasmodial potency determined to fall between 200 and 350 Å^3.[81] The most potent analogue from this series was a bisammonium analogue with a 21-carbon linker and triethylammonium heads (G19 IC_{50} = 0.003 nM).

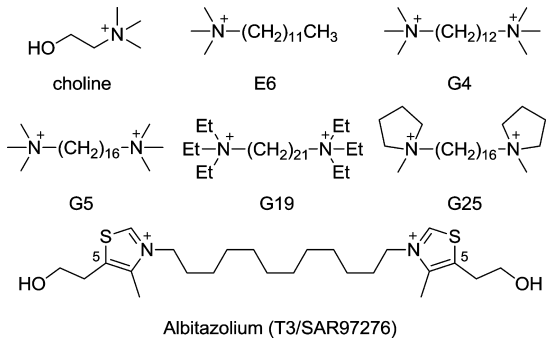

Figure 6. Development of T3/SAR97276.

From the set of potent analogues, G25 was chosen for closer analysis of drug specificity, antiplasmodial activity, and pharmacology. The specificity of G25's inhibitory activity was assessed by comparing the inhibition of de novo biogenesis of PC with that of both phosphatidylethanolamine (PE) and nucleic acids.[82] This study showed that G25 selectively inhibited the incorporation of choline into PC (PC_{50} = 0.4 μM), where inhibition of nucleic acid (NA_{50} = 1.2 μM) and PE (PE_{50} > 100 μM) synthesis occurred at higher concentrations.[83] In addition, the close correlation between PC synthesis and parasite growth inhibition was also re-established. The stage specificity of G25 for the asexual intraerythrocytic parasite life cycle was assessed, with G25 showing the maximal effect on trophozoite-stage parasites (IC_{50} = 0.75 nM),[83] where the majority of PL membrane synthesis takes place.[79] Parasites undergoing schizogony were 10-fold less sensitive to the drug (IC_{50} = 9 nM), and parasites in the ring stage, where little PL biogenesis occurs, were substantially less sensitive (IC_{50} = 160 nM), supporting a PL biogenesis inhibition mechanism.[83]

The susceptibility of laboratory strains and clones of *P. falciparum* was assessed in collaboration with eight independent laboratories, and it was found that G25 retained potency and did not show cross-resistance with known antimalarials (IC_{50} values between 0.2 and 15.3 nM against 3D7, L-16, FCR3, L1, FCB-1, F147, H1, K1, T996, 1G8, W2, D6, and TM90C3B).[83] Analysis of G25's potency in vitro against nine CQ-resistant field isolates of *P. falciparum* from six distinct countries revealed potent activity (IC_{50} values between 7.7 and 20 nM), and further analysis against a panel of 106 *P. falciparum* field isolates from Thailand showed no cross-resistance with the antimalarials used for comparison (CQ, quinine, mefloquine, halofantrine, and artemether). G25 was significantly weaker against mammalian cell lines (U937 macrophage, Jurkat lymphoblast, and MEG-01 megakaryoblast), with growth inhibition occurring only at micromolar concentrations, providing selectivity indexes higher than 300.[83] The potent antiplasmodial activity and selectivity were also supported by the observation that a tritium-labeled analogue of G25 accumulates at almost 180-fold higher concentrations in infected RBCs compared to noninfected RBCs.[84] Accumulation was found to be essentially irreversible, as replacing the supernatant of the suspension of RBCs loaded with compound with fresh medium resulted in drug retention of 95% and 87% after 3 h at 37 and 4 °C, respectively.

Preliminary in vivo experiments with G25 revealed it was fairly toxic to mice and rats (LD_{50} values ranging from 1.4 mg/kg iv (intravenously) to 110 mg/kg po).[85] At high doses, G25 induced a rapid and transient hypoxia as a result of interference with respiratory muscles typified by a decrease in respiration rate and hemoglobin oxygen desaturation.[84] Additional studies conducted on dogs and monkeys revealed low tolerated doses (<0.9 mg/kg). Although toxicity was high, G25 was potent in vivo against *Plasmodium chabaudi* infected mice (ED_{50} = 0.08 mg/kg). The compound was also curative. However, the therapeutic index (TI) was only 17.

G25 was also potent in vivo against the *P. falciparum* FVO strain in *Aotus* monkeys, being curative at doses of 0.2, 0.09, or 0.03 mg/kg (im, intramuscularly) with no signs of recrudescence after a 60-day follow-up. In this animal model the TI was at least 30. At a dose of 0.01 mg/kg, parasitemia initially decreased but then rose again at day 2.5, and at day 7, parasitemia was only detectable in thick blood films, suggesting the dose was approaching the threshold of therapeutic activity.[84]

Despite excellent in vivo activity in multiple models, this compound series suffered from limited oral bioavailability and high toxicity. To address these issues, a new series was developed in which the trialkylammonium moiety was replaced by a thiazolium headgroup,[86] which occurs naturally as vitamin B1. Examination of a series of bis-thiazolium-head analogues

confirmed that the 12-carbon alkyl linker was optimal for potency. In addition, a methoxyethyl substitution in the 5-position of the thiazolium ring produced the highest potency analogues, which combined with the optimized linker provided T3/SAR97276 (Figure 6; *P. falciparum* IC_{50} = 0.65 nM). T3 was highly potent in vivo in *Plasmodium vinckei* infected mice (ED_{50} = 0.2 mg/kg, ip (intraperitoneally)). Subsequent toxicological studies showed a more favorable therapeutic profile (TI > 50).[86] Further in vivo analysis showed equivalent ED_{50} values against high parasitemia infections, and complete cures without recrudescence were obtained at doses 2−4 times the ED_{50} (ip, im, or iv route) as well as with a single injection (6.75 mg/kg).[87] On the basis of the overall pharmacological, biological, ADME (absorption, distribution, metabolism, and excretion), and toxicological data, T3/SAR97276 was selected as a clinical candidate. Regulatory preclinical and phase I studies were carried out successfully by Sanofi-Aventis, and phase II studies were initiated for the treatment of severe malaria (parenteral route) in 2008.[88] In concurrent studies, neutral thioester precursor molecules are being investigated as prodrugs in hopes of developing an orally bioavailable alternative.[87,89] No further development has been reported.

2.4. Dihydrofolate Reductase Inhibitor P218

The de novo synthesis of folate is required for DNA synthesis in *Plasmodium* species. The final step of folate synthesis is the enzymatic reduction of 7,8-dihydrofolate (DHF) to 5,6,7,8-tetrahydrofolate (THF), which is catalyzed by the enzyme dihydrofolate reductase (DHFR). Following the first report of the antimalarial activity of the biguanidine proguanil by Imperial Chemical Industries (ICI) in 1945,[90] cycloguanil (CG, Figure 6) was identified as a potent metabolite formed from proguanil by CYP2C19 metabolism.[91] Cycloguanil is a competitive inhibitor of DHF binding to DHFR. In parallel work, 2,4-diaminopyrimidines were developed as folic acid analogues, leading to the identification of the DHFR inhibitor pyrimethamine[92] (PYR, Figure 7), which has been clinically utilized in combination with sulfadoxine for malaria prophylaxis. Resistance to antifolates occurs from point mutations in the *Pf*DHFR gene. The "stacking" of these mutations due to sequential acquisition in a population leads to increased resistance, with the "quad mutant" containing the N51I, C59R, S108N, and I164L mutations being over 1000-fold more resistant.[93] The S108N mutation causes reduced binding efficiencies to PYR and CG, both having rigid *p*-chlorophenyl substitutions.[71,94] Subsequent mutations diminish binding affinities resulting from protein alterations that preferentially affect the binding of inhibitors with a lesser effect on substrate binding.[95]

Following the observation of the occurrence of resistant mutants to PYR,[96] the Walter Reed Army Institute (WRAIR) identified a cycloguanil analogue, WR99210 (Figure 7), that possessed significant potency against PYR-resistant mutant strains of *P. falciparum*.[97] This compound was later dropped from development due to poor bioavailability and severe gastrointestinal toxicity. To gain understanding of the mode of antifolate resistance for mutants showing diminished antimalarial activity and protein binding affinities, the X-ray cocrystal structures of the wild-type, double-mutant (C59R/S108N), and quadruple-mutant (V1/S) *Pf*DHFR-TS bound to inhibitors were solved.[95a] The structure of the mutant enzyme with inhibitor WR99210 revealed that the flexible side chain of WR99210 is oriented in such a way to avoid steric clash with

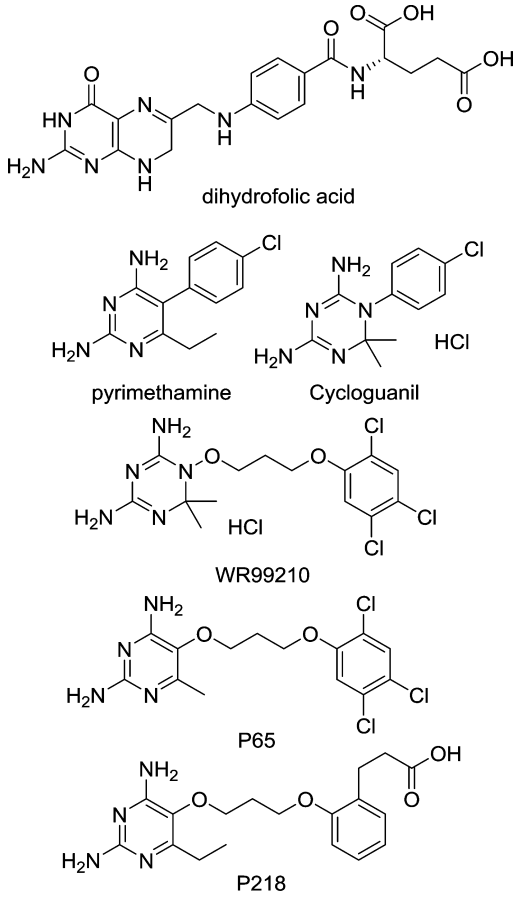

Figure 7. Development of P218.

residue Asn108, whereas steric clashes between the rigid *p*-chlorophenyl side chain of inhibitors PYR and CG cannot be avoided. This observation explained the experimentally observed 20-fold decrease in affinity for PYR in the double mutant as compared to only a 2-fold decrease for WR99210 affinity.

On the basis of this discovery, a structure-based approach was implemented to discover novel DHFR inhibitors.[98] The bioavailability of WR99210 was determined to be less than 1%, with cell-based Caco-2 permeability assay suggesting the low bioavailability was likely due to poor intestinal permeability. Substantial differences in basicity were believed to be a major contributing factor, where triazines WR99210 and CG are more basic (pK_a = 10−11) than pyrimidines such as PYR (pK_a = 6−7) and are expected to be fully protonated in the gastrointestinal tract, thus hindering absorption.[99] A hybrid molecule combining the flexible side chain of WR99210 and the pyrimidine of PYR (Figure 7, P65) was designed with the intention of combining the potency against resistant mutants displayed by WR99210 and the superior bioavailability of PYR. P65 had high bioavailability in rats (83%), which confirmed the value of the pyrimidine moiety for enhanced bioavailability. Importantly, P65 was also a potent inhibitor of the quadruple-mutant *Pf*DHFR (k_i = 5.6 nM). The cocrystal structure of P65 bound to quadruple-mutant *Pf*DHFR-TS was solved, and the active-site binding interaction was found to be identical to that of WR99210. However, when P65 was compared to WR99210 in the DHFR quadruple-mutant *Pf* strain (V1/S), a 200-fold lower activity was observed (IC_{50} = 3490 and 18 nM, respectively).

The optimal binding interactions and pharmacokinetic properties of the pyrimidine core and the ideal flexible five-atom linker arm left only the trichlorophenyl ring of P65 open for optimization. A charge-mediated hydrogen-bonding interaction between the α-carboxylate of the dihydrofolate substrate and a conserved Arg (Arg122 in *Pf*DHFR, Arg70 in human DHFR) residue was targeted to improve potency, a strategy that had been employed previously.[100] Furthermore, inhibitor selectivity was targeted by taking advantage of species-dependent amino acid differences in the vicinity of the conserved Arg, which could be exploited to prevent binding to the human enzyme. On the basis of this hypothesis, a total of 14 compounds, substituting the 2′-chloro or the 3′-hydrogen of the trichlorophenyl group, were produced. Compound P218 was a potent inhibitor of the quadruple-mutant *Pf* (V1/S) in vitro (EC_{50} = 56 nM), almost a 100-fold improvement over P65.

The binding of P218 to *Pf*DHFR-TS and to human DHFR was examined in cocrystal structures of the inhibitor-bound enzyme.[98] When bound to quadruple-mutant *Pf*DHFR, the newly introduced carboxylate of P218 makes two charge-mediated hydrogen bonds with Arg122. In contrast, it has no interaction with Arg70 in the human DHFR. Furthermore, unlike PYR, P218 binds to *Pf*DHFR within the envelope of the dihydrofolate substrate itself. P218 binds to *Pf*DHFR in a biphasic manner, in which a rapidly equilibrating initial binding step is followed by a slow enzyme isomerization to form a higher affinity complex with overall slow-on/slow-off kinetics. Importantly, the binding of P218 to human DHFR was determined to be poor, as predicted from the structures.

In addition to the high potency against PYR-resistant *P. falciparum* (V1/S) in vitro, P218 was highly potent in vivo against both *P. chabaudi* in mice (ED_{90} = 0.75 mg/kg) and quadruple-mutant *P. falciparum* in severe combined immunodeficiency (SCID) mice (ED_{50} = 0.3 mg/kg, ED_{90} = 1 mg/kg). P218 possessed good bioavailability in rats (46%), at 30 mg/kg, a reasonable half-life (7 h), and minimal distribution to the brain. P218 was not genotoxic in the Ames test, did not significantly reduce hERG currents in CHO cells at concentrations up to 30 μM, and did not inhibit cytochrome P450 enzymes at concentrations up to 30 μM. Exploratory repeat-dose oral toxicity set the NOAEL at approximately 100 mg/kg/day in the rat. P218 is currently in preclinical development.

2.5. ELQ-300

While glycolytic metabolism is recognized as the fundamental source of energy production in the *Plasmodium* parasites, the electron transport chain (ETC) is essential for parasite survival.[101] A major evident role of the ETC in the parasite is to drive the biosynthesis of pyrimidine, which is required for DNA synthesis as pyrimidine scavenging is absent in *Plasmodium*. The parasite ETC has a minimalist composition compared to that of bigger eukaryotes, missing the NADH:ubiquinone oxidoreductase (complex I) altogether, while complexes II–IV are expressed in simplified forms. The seemingly stark differences in the ETC from parasites to humans make the ETC an attractive target for the identification of selective compounds for the parasite over the host. Targeting the ETC has been validated with the clinical success of atovaquone, which inhibits the parasite cytochrome bc_1 complex.[102]

The quinolone endochin (Figure 8) was first described in 1948[103] as possessing activity in both the prophylactic and curative models of sporozoite-induced *Plasmodium cathemerium* in canaries. However, it was subsequently found to be

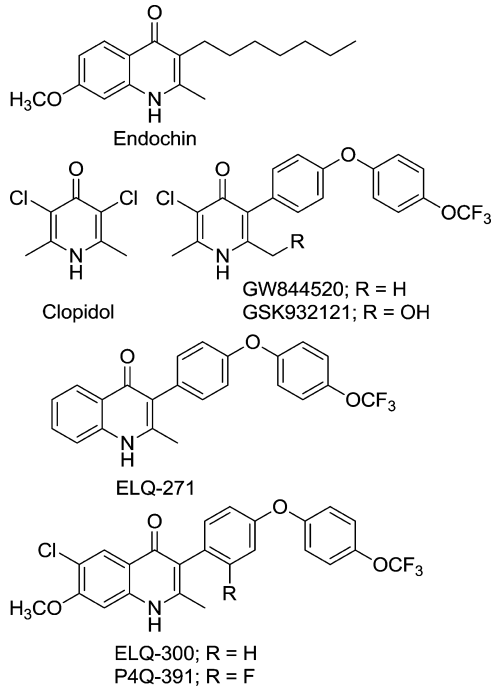

Figure 8. Development of ELQ-300.

ineffective against human malarias.[104] Like atovaquone, endochin blocks mitochondrial respiration in red blood cells infected with *Plasmodium*.[105] Endochin and its direct analogues suffer from poor pharmacological properties, including rapid metabolism in human liver microsomes and poor aqueous solubility, which has limited the development of the series.[105,106]

In the late 1960s, the structurally related anticoccidial drug clopidol (Figure 8) was reported to possess antimalarial activity in a number of animal models, acting through inhibition of *Plasmodium* mitochondrial electron transport.[107] The introduction of a lipophilic side chain at C-5 on clopidol (GW844520, Figure 8) provided significant improvements in potency in vitro against *P. falciparum* and in vivo against *P. yoelii*,[108] which is thought to act by inhibition of the *Plasmodium* cytochrome bc_1 complex. However, GW844520 does not share cross-resistance with atovaquone and does not show synergism with proguanil, which suggests either a different binding mode or a different mechanism of action compared to that of atovaquone. On the basis of good in vivo potency and efficacy in the mouse *P. yoelii* model, GW844520 was tested in *Aotus* monkeys infected with *P. falciparum*. The compound was completely curative after oral administration of seven daily doses of 10 mg/kg.[109] Although the bioavailability of GW844520 was excellent at low dose (72% at 0.5 mg/kg in mouse),[110] it dropped substantially when the dose was escalated 10-fold (~20% at 10 mg/kg), presumably due to low aqueous solubility (<0.24 μM).[109] Introducing a hydroxymethyl group to the C-6 position gave GSK932121 (Figure 8), which possessed significantly increased solubility and improved bioavailability, while maintaining the in vitro and in vivo antimalarial activity.[111] GSK932121 progressed into

dx.doi.org/10.1021/cr500543f | *Chem. Rev.* 2014, 114, 11221–11241

phase I clinical trials, but was withdrawn after unexpected deaths were observed in preclinical studies in rats, which were attributed to the inhibition of mammalian mitochondrial cytochrome bc_1.[109]

A subsequent program, building from both the experience with endochin and the GSK work, combined the endochin nucleus[105,106,112] with the optimized diphenyl ether side chain at the 3-position of GW844520[108] to arrive at ELQ-300 and P4Q-391 (Figure 8).[113] These compounds had excellent in vitro antiplasmodial activity (EC_{50} values between 1.3 and 13.6 nM for ELQ-300 and from 3.18 to 32.3 nM for P4Q-391) against a panel of *P. falciparum* strains, including chloroquine-sensitive strains (3D7 and D6), multi-drug-resistant strains (Dd2, W2, and isolates from Southeast Asia), and the atovaquone-resistant clinical isolate TM90-C2B, which carries a mutation in the cytochrome *b* gene.[114] Cellular studies designed to ensure selectivity for *Plasmodium* cytochrome bc_1 over the human protein revealed a clear SAR where adding substituents on the quinolone benzenoid ring reduced inhibitory activity against the human cytochrome bc_1 complex when an IC_{50} = 1.99 μM was established for unsubstituted ELQ-271 (Figure 8) compared to IC_{50} > 10 μM for both ELQ-300 and P4Q-391, containing both halogen and methoxy substitutions. ELQ-271 also caused a concentration-dependent decline in ATP levels in mammalian cell lines (EC_{50} values from 7.4 to 15.4 μM), suggesting inhibition of the mitochondrial electron transport, whereas ELQ-300 had no measurable effect at concentrations of 10 μM or higher. ELQ-300 and P4Q-391 potently inhibited *P. falciparum* cytochrome bc_1 (IC_{50} = 0.58 and 1.06 nM, respectively), demonstrating high selectivity over the mammalian proteins and suggesting low potential for side effects arising from inhibition of human cytochrome bc_1. Both ELQ-300 and P4Q-391 were highly potent in *P. berghei* infected mice (ED_{50} = 0.016 and 0.3 mg/kg, respectively), and cures were achieved with no recrudescence at a dose of 1 mg/kg. ELQ-300 was also potent against *P. falciparum* infected SCID mice (ED_{90} = 6 mg/kg/day).[115]

ELQ-300 was found to be a slow-acting drug with a delayed parasite reduction ratio similar to that of atovaquone.[113] Potential for drug resistance was evaluated by selecting for resistant clones in the presence of atovaquone (10 nM) or ELQ-300 (150 nM) under continuous drug pressure. While drug-resistant parasites could be reliably selected with atovaquone, no resistant parasites were observed with ELQ-300, predicting a lower propensity for ELQ-300 to induce resistance in malaria parasites than atovaquone.

Both compounds were highly potent in blocking invasion of the sporozoite stage of *P. berghei* to HepG2 hepatoma cells in vitro (EC_{50} = 1 and 5 nM for ELQ-300 and P4Q-391, respectively). Likewise, ELQ-300 potently blocked infection of primary hepatocytes from rhesus monkeys by *Plasmodium cynomolgi* sporozoites (IC_{50} = 100 nM), which resemble the liver stage of the human malaria parasite *P. vivax*.[116] Furthermore, both ELQ-300 and P4Q-391 were highly effective at blocking infection of mice by *P. berghei* sporozoites in vivo at doses as low as 0.03 mg/kg. The compounds were also determined to be active against sexual stages of the parasite life cycle, with ELQ-300 preventing development of early-stage gametocytes past stage III at a 0.1 μM dose. ELQ-300 was also found to have activity against mosquito stages of the parasite, including the inhibition of ookinete and oocyst formation.[113]

Assessment of the physiochemical properties of ELQ-300 and P4Q-391 suggested that the solubility would limit oral absorption; however, when evaluated in vivo, both compounds exhibited good bioavailability (~100%) at low doses with a decrease observed at higher doses due to solubility-limited absorption. Following intravenous administration to mice, both compounds exhibited moderate volumes of distribution (~1.2 L/kg) and low clearance (~0.7 mL/min/kg) with half-lives greater than 15 h, as was predicted from the high stability when they were exposed to liver microsomes. ELQ-300 is currently in investigational new drug (IND) enabling studies.

2.6. PNP Transition-State Analogue BX4945

Plasmodium parasites are purine auxotrophs that depend exclusively on salvaged purine bases from the host for DNA and RNA synthesis.[117] The purine salvage pathway in *P. falciparum* utilizes hypoxanthine, the common precursor for all purine nucleotides in the parasite,[118] formed either in erythrocytes or in parasites by sequential enzymatic transformations by adenosine deaminase (*h*ADA, *Pf*ADA) and/or purine nucleoside phosphorylase (*h*PNP, *Pf*PNP).[119] Depletion of hypoxanthine by the addition of xanthine oxidase to *Plasmodium* culture media inhibits parasite growth,[120] and PNP is critical to parasite viability.[121] Therefore, inhibition of PNP was targeted for novel antimalarials.

Early studies investigating the biochemical mechanism of nucleoside cleavage catalyzed by PNP gave insight into the transition state and provided a design rationale for PNP inhibitors.[122] Evaluation of the kinetic isotope effects of PNP revealed that the enzyme stabilized a ribooxocarbenium ion produced by protonation of N7 of the purine base. The involvement of N7 in the enzymatic mechanism was supported by X-ray crystallographic studies that revealed a hydrogen bond between N7 and a highly conserved asparagine residue, which would stabilize the negative charge accumulation on the purine ring during glycosidic bond cleavage.[123] In the reaction, inosine is slowly hydrolyzed to hypoxanthine and ribose with little contribution from the nucleophilicity of phosphate.[124] While ribose is released in the process, hypoxanthine is sequestered by noncovalent tight-binding interactions with PNP (K_d = ca. 1 pM), allowing for characterization of the PNP−hypoxanthine complex and identification of one hypoxanthine equivalent per protein homotrimer.[125]

Immucillins (Imm's, Figure 9) were conceptualized as inhibitors incorporating features of both guanine and hypoxanthine but with elevated pK_a values at the N7 position. In addition, the ribooxocarbenium ion is mimicked by an iminoribitol moiety. Imm-H and Imm-G were found to be slow-onset, slow-release, tight-binding inhibitors of PNP with exceptional affinity for the human and bovine isoforms (K_i* = 72 and 29 pM, respectively).[125]

To evaluate if PNP inhibition could affect parasite survival, the immucillins were tested in vitro against *P. falciparum* and found to have potent growth inhibitory activity (IC_{50} = 35 and 50 nM for Imm-H and Imm-G, respectively).[126] The affinities of the immucillins, and their deoxyribose analogues, were weaker against *Pf*PNP (K_i* = 0.6 and 0.9 nM for Imm-H and Imm-G, respectively[127]) than the human enzyme.[126] To confirm whether the depletion of hypoxanthine caused growth inhibition, the authors supplemented the media with hypoxanthine and found that parasite growth could be rescued with concentrations greater than 20 μM, providing parasite viability of ~50% compared to the control under otherwise suppressive concentrations of Imm-H (10 μM). Further studies found that the inhibition of both human and *P. falciparum*

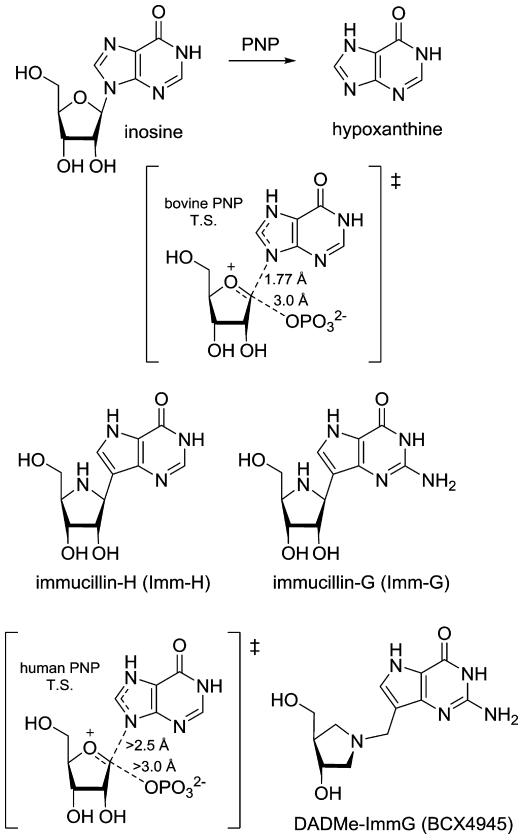

Figure 9. Development of BCX4945.

PNPs blocks the conversion of radiolabeled [^{3}H]inosine into hypoxanthine and induces purine starvation, resulting in growth inhibition.[126]

On the basis of the observation of stronger binding affinities for bovine compared to human PNPs, the team re-examined the transition-state structure of human PNP to design a second-generation inhibitor.[128] Closer evaluation of kinetic isotope effects for the substrate with human enzyme revealed a more dissociated transition state than observed in bovine PNP with greater separation between the ribosyl group and the departing purine ring. Along with the increased transition-state bond length comes an increased cationic character at C-1′. Taking these two aspects into consideration allowed for the design of DADMe-immucillins (Figure 9).

The second-generation immucillins possessed good oral bioavailability in mice, much weaker mammalian toxicity,[129] and strong binding to both the human and parasite PNPs (K_d = 7 and 890 pM, respectively).[130] BCX4945 (DADMe-ImmG) was chosen for further study.[131] BCX4945 was reasonably active against *P. falciparum* in vitro at physiologically relevant hypoxanthine concentrations (<10 μM)[132] with good potency for 3D7, Dd2, and FVO (IC_{50} = 164, 130, and 202 nM, respectively).[131] BX4945 had modest in vivo efficacy as *P. falciparum* (FVO strain) infected *Aotus* monkeys (50 mg/kg, po) dosed twice daily for 7 days cleared infection between the fourth and the seventh day of treatment. However, all treated monkeys recrudesced following treatment. No signs of toxicity were seen during the 30 day study period. Pharmacokinetic analysis of BCX4945 in both uninfected and infected *Aotus* monkeys revealed moderated oral bioavailability (28%) with good peak plasma concentrations (C_{max} = 15 μM) in the uninfected animal. The half-lives were not affected by *P. falciparum* infection.

3. IDENTIFICATION OF NOVEL ANTIMALARIALS VIA HIGH-THROUGHPUT SCREENING (HTS)

3.1. Triazolopyrimidine DSM265

Following proof that the de novo biosynthesis of pyrimidine is indispensable in the malaria parasite, inhibition of this pathway became a focus of antimalarial drug discovery. The fourth step is the flavin mononucleotide-dependent conversion of dihydroorotate (DHO) to orotate that is catalyzed by dihydroorotate dehydrogenase (DHODH). One series of *Pf*DHODH inhibitors were discovered by high-throughput screening using a DHODH enzymatic assay.[133] A library of 220 000 molecules were screened to identify 1249 compounds that inhibited the enzyme by at least 60% at 3 μM, giving a hit rate of 0.6%. Hit compounds were retested against both *Pf*DHODH and human DHODH to narrow the field of active compounds to those with good potency (IC_{50} < 0.6 μM) that were selective for the parasite. The hit compounds were then re-evaluated in kinetic enzyme assays, identifying a number of compounds that reversibly inhibited *Pf*DHODH at nanomolar concentrations.

One of the hit compounds identified through the HTS campaign was triazolopyrimidine DSM1 (Figure 10), which potently inhibited *Pf*DHODH (IC_{50} = 47 nM) with >5000-fold

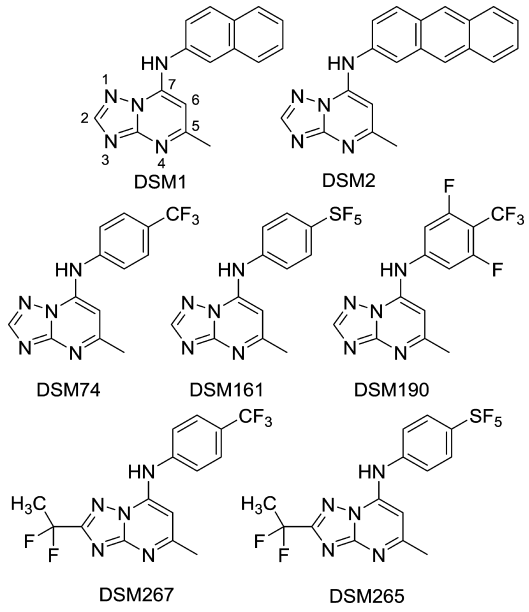

Figure 10. Development of DSM265.

selectivity versus the human enzyme.[134] DSM1 was also potent against *P. falciparum* strain 3D7 in culture (EC_{50} = 80 nM) and against multiple-drug-resistant *P. falciparum* strain Dd2 (EC_{50} = 140 nM) without inhibiting the growth of mouse cell line L1210 at concentrations up to 10 μM. Early structure−activity studies revealed that the optimal substitution on the pyrimidine ring was a CH_3, with a 4-fold loss of potency observed for C_2H_5 and CF_3 substitutions and when a second CH_3 was substituted for the remaining hydrogen. A 60-fold loss in potency was observed when a CH_3 was added to the exocyclic amine to give the corresponding tertiary amine. Introduction of heteroatoms on, or within, the naphthyl ring also resulted in a loss of potency. When the 2-naphthyl was switched to a 1-naphthyl,

dx.doi.org/10.1021/cr500543f | *Chem. Rev.* 2014, 114, 11221−11241

potency was reduced by 2 orders of magnitude. Replacement of the naphthyl with a phenyl ring also caused a significant reduction in potency, whereas a larger anthracyl substitution was well tolerated (DSM2).

Steady-state kinetic analysis showed a linear increase in IC_{50} for DSM1 with increasing CoQ_D concentrations, which is expected for a competitive tight-binding inhibitor, and the K_i was determined to be 15 nM. Pre-steady-state stopped flow kinetics demonstrated that DSM1 inhibited the oxidative half-reaction (k_{ox}), preventing the transfer of electrons from $FMNH_2$ to CoQ_D where the DHO-dependent reductive half-reaction (k_{red}) was unaffected. In addition, site-directed mutagenesis of residues in the inhibitor binding site of *Pf*DHODH (F227A and R265A) increased the IC_{50} of DSM1 by 940-fold and 130-fold, respectively, providing convincing evidence that DSM1 binds to this site, which is poorly conserved between *P. falciparum* and human DHODH.

The early leads DSM1 and DSM2 were inactive in vivo in *P. berghei* infected mice at a dose of 100 mg/kg.[135] Examination of the amino acid sequence differences between the inhibitor binding sites of *Pf*DHODH and *Pb*DHODH revealed two differences (M536 and G181 in *Pf*DHODH and V536 and S181 in *Pb*DHODH).[136] These differences were enough to drop the potency against *Pb*DHODH for DSM1 and DSM2 5-fold and 66-fold relative to that against *Pf*DHODH, partially explaining the observed lack of efficacy.[135] The pharmacokinetics of DSM1 and DSM2 were analyzed at a single oral dose of 50 mg/kg in uninfected mice to determine if the lack of efficacy was exacerbated by poor bioavailability. The plasma levels for both compounds reached 1−3 μM concentrations in plasma 30 min after administration. However, DSM1 concentrations declined by 4 h postdose, whereas DSM2 sustained plasma exposures between 1 and 3 μM over 4 h. The lack of efficacy of DSM1 in *P. berghei* infected mice was attributed to reduced exposure upon repeat administration coupled with reduced inhibitor potency.[135]

To improve the pharmacokinetics while maintaining activity in *P. berghei*, a set of 40 compounds replacing the naphthyl group were produced on the basis of the Topliss approach.[137] The compounds were tested for activity against three homologues of recombinant enzyme (*Pf*DHODH, *Pb*DHODH, and *h*DHODH) and against *P. falciparum* parasites.[135] As established previously, substituting the naphthyl for the unsubstituted phenyl group resulted in a complete loss of activity. Analogues with single substituents in the *ortho* position of the ring were inactive, while *meta*-substituted analogues offered some activity. The most potent singly substituted compounds from the series contained *para* substituents where larger hydrophobic groups displayed better activities: CF_3 > Br > OCF_3 > CH_3, NO_2, F, Cl. The best activities were observed with combinations of substitutions in the *meta* and *para* positions of the phenyl ring. Preferential binding to *Pf*DHODH over *Pb*DHODH was observed for most of the compounds in the series with the exception of *p*-CF_3-phenyl-substituted analogue DSM74 (Figure 10), which was found to be an equipotent inhibitor of the two enzymes, but around 5-fold less potent than DSM1 and DSM2.

Several of the compounds were tested for metabolic stability in human liver microsomes. Both DSM1 and DSM2 had high rates of degradation, while those analogues with a *p*- or *m*-halogen, or other nonoxidizable substituent, possessed greater stability.[135] DSM74, which had superior microsomal stability, was tested in vivo in mice as single oral doses of 20 or 50 mg/kg. It gave peak plasma concentrations of 8 and 28 μM, respectively, and plasma concentrations were maintained above 1 μM for 16 h with a half-life of 3 h following the 50 mg/kg dose, a substantial improvement over DSM1 and DSM2. Analogue DSM74 reduced parasitemia 95% in *P. berghei* infected mice (50 mg/kg, twice daily for 4 days).

Solving the X-ray crystal structure of *Pf*DHODH bound to inhibitors revealed that the binding pocket for the aryl amine is narrow and completely hydrophobic.[138] This explained the observation that *ortho* substitutions of the aniline ring are not tolerated. Subsequent rational design to further optimize the aryl amine moiety centered on aliphatic substitutions at the *para* position of the aniline.[139] The analogue containing a *tert*-butyl substitution proved to be the most potent, followed by isopropyl and straight chain aliphatic substitutions. Extension of the aliphatic chain confirmed the limited size of the pocket because extending the chain past five carbons resulted in decreases in potency, as did the substitution of the aniline for aliphatic rings. Exploration of fluorinated groups at the *meta* and *para* positions of the aniline identified an analogue with a 2−3-fold increase in potency, substituting a SF_5 for the CF_3 of DSM74, giving DSM161 (Figure 10). Alternatively, addition of two *m*-fluorines to DSM74 provided a moderate enhancement in potency (DSM190).

Microsomal modeling of this set of analogues predicted high metabolic clearance for the most potent analogues due to rapid metabolism in liver microsomes, whereas slightly less potent analogues DSM161 and DSM190 displayed improved metabolic stability.[139] The in vivo pharmacokinetics of the lead compounds were improved with a single oral dose of 20 mg/kg, giving both high C_{max} values (31 and 34 μM in rats, respectively) and prolonged half-lives (~20 h in mice and 33 and 18 h in rats, respectively). The oral bioavailability in rats was high (>100%). In vivo efficacy studies with *P. berghei* infected mice showed the improved compounds were potent (ED_{50} for DSM161 and DSM190 was 17 and 10 mg/kg, respectively), although neither compound was curative.

Further medicinal chemistry efforts to optimize the scaffold focused on the previously unexplored C2 position of the triazolopyrimidine core. A variety of structural variations were examined, including varying the chain length, branching, electronic effects, heteroatom effects, polarity effects, and donor and acceptor hydrogen-bonding effects. The goal was to find extra interactions with the flavin mononucleotide (FMN) cofactor.[140] Branched alkyl groups at C2 were generally well tolerated with the exception of isobutyl, suggesting that the binding pocket is wide enough to accept steric bulk on the atom adjacent to C2 but narrows beyond the second atom. Lower potency was observed with a carbon spacer placed between the ether linkage and C2 or with the incorporation of a free alcohol. A complete loss of activity was observed with analogues containing a free amine, as expected with the lipophilic binding pocket. The most potent analogues for both *Pf*DHODH inhibition assays and whole cell assays contained an unbranched haloalkyl group at C2 as exemplified by DSM267 and DSM265 (Figure 10). These analogues displayed potencies against *Pf*DHODH equivalent to those originally found in DSM1, but failed to maintain equal potency with *Pb*DHODH.

In vitro modeling of DSM265 and DSM267 predicted good oral absorption (MW < 430, <2 H bond donors, <6 H bond acceptors, polar surface area <90 Å^2), but solubility was only moderate (30−60 μM for DSM265 and 70−140 μM for

DSM267).[140] Also, plasma protein binding to both human and mouse plasma was very high for DSM265 (99.9% and 99.6%, respectively) and slightly lower for DSM267 (98.8% and 97.4%, respectively). Microsomal modeling predicted low predicted intrinsic clearance (CL_{int} < 6 and 10 μL/min/mg for human and mouse liver microsomes, respectively). The pharmacokinetics of new frontrunner compounds were assessed in mice and rats. Both had good exposure following a single oral dose. C_{max} and AUC values were found to increase proportionally over the full dose range (0.4−50 mg/kg), but the increase was diminished for the 50 mg/kg dose for DSM265. Following iv dosing in rats, DSM265 displayed low clearance (4−6 mL/min/kg), a moderately high volume of distribution (3−6 L/kg), and a long half-life (10−13 h). DSM267 showed higher clearance (13−23 mL/min/kg), a similar volume of distribution (3 L/kg), and a shorter half-life (4−6 h). Following oral administration of a 2 mg/kg dose, both compounds exhibited good oral bioavailability (~60% for DSM265 and >97% for DSM267) and long half-lives (12 h for DSM265 and 6 h for DSM267). Due to lower sensitivities observed against *Pb*DHODH, the compounds were tested in the *P. falciparum* SCID mouse model where both DSM265 and DSM267 were efficacious when dosed once daily for 4 days (ED_{90} values of 8 and 26 mg/kg, respectively). DSM265 showed a clear potency advantage in vivo, while parallel pharmacokinetics displayed similar exposures for both compounds, suggesting the differences in efficacies were a direct result of differences in antimalarial potencies. Ultimately, DSM265 was chosen as the candidate for development and is currently in phase I clinical trials and is being prepared for a phase IIA trial in Peru to begin in late 2014 (www.mmv.org).

3.2. Spiroindolone NITD609/KAE609

Phenotypic screening[141] of a library of about 12 000 pure natural products and related compounds at Novartis resulted in the identification of 275 primary hits with <1 μM activity against *P. falciparum*. Compounds that showed cross-resistance with strains resistant to known antimalarials and compounds that showed >50% viability inhibition of mammalian cells at 10 μM were discarded, leaving 17 validated hits. An examination of their physiochemical and pharmacokinetic properties led to the selection of spiroazepineindole **11** (Figure 11) as a lead for optimization.[142] Spiroazepineindole **11** was resynthesized using a Pictet−Spengler cyclization providing **11** in a ~9:1 diastereomeric ratio for which the major enantiomer set was resolved, and the X-ray crystal structures were solved to determine the conformations of the enantiomers to be (1*R*,3*S*) and (1*S*,3*R*). The individual enantiomers displayed dramatically different activity against *P. falciparum* (NF54) where the (1*R*,3*S*)-enantiomer (EC_{50} = 10 nM) was 250-fold more potent than the (1*S*,3*R*)-enantiomer. On the basis of this lead, spiroindolone **12** was synthesized and resolved, providing all four possible stereoisomers (**12a**−**d**). The most active stereoisomer was **12a** (EC_{50} = 9 nM), with the (1*R*,3*S*)-conformation. Subsequent structure−activity relationship studies revealed that the spirocenter was essential. In extended studies, replacement of the 5′-bromide of **11** negatively affected the potency, with the exception of the 5′-chloro analogue, which provided an optimal balance among potency, favorable PK, and synthetic accessibility. Simplification of the molecule by removing the C3 methyl substituent did not affect the potency of the seven-membered ring azepine. However, the corresponding tetrahydro-β-carboline (spiroindolone) analogue

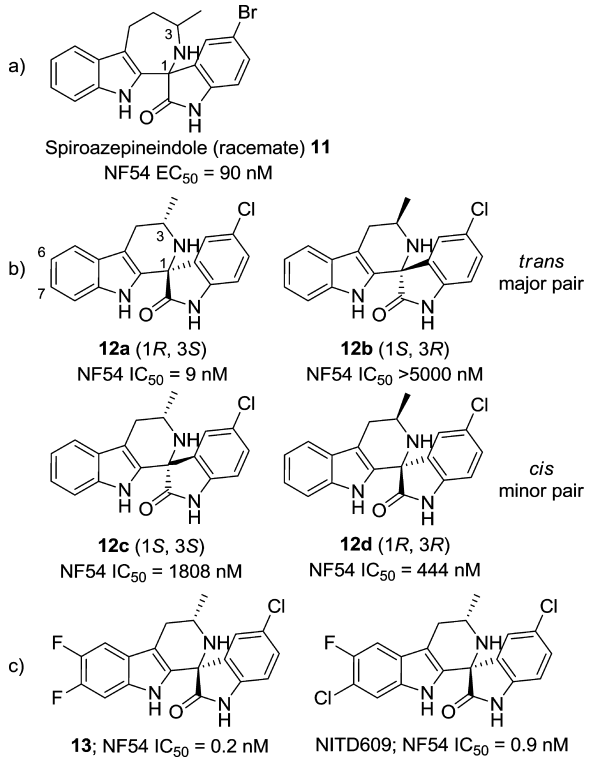

Figure 11. Development of NITD609/KAE609.

lacking the C3 methyl was 5-fold less potent than the analogue with the methyl present. Any other modification at C3 was deleterious, including increasing the steric bulk to *gem*-dimethyl, hydroxymethyl, *n*-propyl, or methyl esters.

The spiroindolones possessed a good physiochemical profile for development. There was no cytotoxicity against several human cell lines and no significant binding in a panel of human receptors, kinases, and ion channels (IC_{50} > 10 μM).[142] In addition, the spiroindolones displayed low cardiotoxicity potential in hERG binding and patch clamp assays and no genotoxicity potential in the Ames and micronucleus tests.[143] The enantiomers were found to have significant differences in both metabolic stability and CYP450 inhibition, with the less potent enantiomers (1*S*,3*R*) displaying superior metabolic stability, low to medium clearance, and minimal CYP450 inhibition. On the other hand, the more potent (1*R*,3*S*)-enantiomers generally had poor microsomal stability and high clearance and inhibited CYP 2C9. To address the metabolic stability issue, substitutions were made at C6 and C7 of the unsubstituted benzene ring of the tricyclic indole, as these were considered to be the most likely sites for metabolism. Installation of a single fluorine at the 6-position provided a slightly more potent analogue (EC_{50} = 3 nM) with no advantage in terms of CYP 2C9 inhibition or in vitro metabolic stability. However, unexpectedly, this analogue provided nearly a 2-fold enhancement in clearance in vivo over **12a**. When a chlorine atom was installed at the 7-position, the active enantiomer showed an improvement in microsomal stability, a 3-fold improvement in potency, and less inhibition of CYP 2C9. The combination of these two substitutions gave NITD609 and **13**, both possessing subnanomolar potency against the parasite, enhanced metabolic stability, and decreased CYP 2C9 inhibition.

dx.doi.org/10.1021/cr500543f | *Chem. Rev.* 2014, 114, 11221−11241

The in vivo PK profiles of **12a** and **13** were then investigated to establish in vitro to in vivo correlations.[142] The iv administration of **12a** gave moderate total systemic clearance (55% hepatic blood flow), a moderate volume of distribution (0.91 L/kg), a short half-life (0.42 h), and a relatively low exposure (3.88 μM h), resulting in a modest bioavailability (13%). On the other hand, iv administration of **13** gave a lower systemic clearance (~10% hepatic blood flow), a higher volume of distribution (1.60 L/kg), a longer half-life (2.94 h), a higher peak plasma concentration (8.32 μM), and an 18-fold increase in exposure (71.44 μM h), resulting in an improvement in bioavailability (53%). In *P. berghei* infected mice a single oral dose of 30 mg/kg of **12a** reduced parasitemia on day 3 by more than 99% and prolonged the mouse survival time to 11 days. **13** showed a modest improvement, prolonging survival to 12 days. No enhancement in efficacy was observed when the doses were escalated to 100 mg/kg, suggesting they had already reached maximal efficacy. In the 3 day dosing schedule, **13** extended survival to 17 and 30 days at doses of 10 and 30 mg/kg, respectively. Cures were observed for four out of five mice at the higher dose.

Continued efforts toward the development and characterization of spiroindolones focused on the evaluation of analogue NITD609 (Figure 11).[144] NITD609 was highly potent against a panel of seven strains of *P. falciparum* resistant to known antimalarials. NITD609 was also active against fresh isolates of *P. falciparum* and *P. vivax*[145] with EC_{50} values consistently lower than 10 nM. *Plasmodium* parasites displayed the same sensitivity at all stages of the asexual life cycle, although schizonts seemed to be slightly more sensitive. On the basis of in vitro experiments, NITD609 appeared to be faster acting than PYR, but it was not as rapid as artemether. A separate assay evaluating protein synthesis by measuring the incorporation of ^{35}S-radiolabeled methionine and cysteine revealed that protein synthesis was blocked within 1 h, an effect also observed with known protein translation inhibitors anisomycin and cyclohexamide. In addition to asexual-stage activity, NITD609 possessed gametocytocidal activity for early to late gametocytes.[146]

The pharmacokinetic and safety profiles of NITD609 supported continued drug development. Mammalian cell cytotoxicity was weak in vitro against cell lines of neutral, renal, hepatic, or monocytic origin.[144] Cardiotoxicity risk was found to be low in hERG binding and patch clamp assays (IC_{50} > 30 μM). No mutagenic activity was observed in a miniaturized Ames assay.[143] Finally, no significant binding was found in a panel of human G-protein coupled receptors, enzymes, and ion channels. Male rats tolerated continuous daily doses of NITD609 for 14 days, with exposure between 76 and 145 μM h, without adverse events or notable histopathological findings. Taken together with the in vitro data, this defines a safety profile acceptable for an antimalarial drug.

NITD609 had strong pharmacokinetic performance in mice and rats, including low total systemic clearance, a long half-life ($t_{1/2}$ = 10 and 27.7 h, respectively, at ~25 mg/kg dose), and excellent bioavailability (100%)—a profile consistent with once daily oral dosing. NITD609 was highly efficacious and potent in the *P. berghei* mouse model ($ED_{50/90/99}$ = 1, 3, and 5 mg/kg) and curative after either a single oral dose of 100 mg/kg or three daily doses of 30 mg/kg. NITD609 successfully completed phase Ia and Ib trials in 2013 and has just completed phase II clinical trials.[147] The drug is currently being recruited for a second trial with the primary outcome of a complete cure rate without recrudescence at day 29 following a single dose (ClinicalTrials.gov identifier NCT01860989).

An effort parallel to clinical development was focused on discovering the target of NITD609. Resistant mutants of *P. falciparum* were selected by applying drug pressure to a cultured clone of Dd2 at increasing sublethal concentrations of NITD609.[144] Resistant mutants with 7−24-fold potency shifts appeared after 3−4 months of constant drug pressure. NITD609-selected parasites were found to be stable, as no evidence of revertants was observed 4 months following removal of drug pressure. The genome of each resistant mutant was sequenced using a high-density tiling array.[148] After the hybridization data were compared to those of the parent Dd2 clone, 27 total differences were identified among the 6 generated mutants, with 7 mapping to a single gene, *Pfatp4* (*PF*L0590c), with one strain exhibiting a copy number variant that encompassed the *Pfatp4* locus, suggesting that spiroindolones specifically select for mutations in *Pfatp4*. The resulting gene product of the *Pfatp4* gene has been reported as a cation-transporting P-type adenosine triphosphatase (ATPase) (*Pf*ATP4)[149] from a family of ATP-dependent transporters that are ubiquitous in eukaryotic organisms.[150] A *Pf*ATP4−GFP (green fluorescent protein) construct suggested that *Pf*ATP4 is localized to the parasite plasma membrane throughout the intraerythrocytic life cycle.[144] This finding was supported by the observation that a fusion protein in late-stage segmented schizonts displayed fluorescence surrounding developing daughter merozoites. Immunofluorescence data also support the localization of *Pf*ATP4 to the plasma membrane.[149b] Characterization of ion levels in the *Pf*ATP4 mutants suggested that Na^+ efflux from the parasite is perturbed by the resistance-conferring mutations.[151] Disruption of parasite Na^+ efflux occurs with roughly the same potency as inhibition of parasite proliferation, strengthening the likelihood that *Pf*ATP4 is the molecular target of NITD609.

3.3. Imidazolopiperazine GNF156/KAF156

A high-throughput screening campaign of a 1.7 million compound library at Novartis identifying compounds inhibiting growth of the asexual stage of *P. falciparum* resulted in the identification of 5973 active compounds showing EC_{50} values of <1.25 μM. Of these, 648 had EC_{50} values of <100 nM, of which >80% were reconfirmed.[141] From this set, GNF−*Pf*-5069 (Figure 12) was identified as one of three hit imidazolopiperazine analogues that displayed potency against both 3D7 and W2 *P. falciparum* strains with a good selectivity index (>20:1) when compared to the mammalian Huh7 cell line.[152] Hit compound 5069 was found to have high solubility (>175 μM at pH 6.8), to be inactive (IC_{50} > 10 μM) against drug-affected CYP450 isoforms, and to possess moderate hERG inhibition activity (IC_{50} = 19 μM). Poor plasma exposure from the oral route was identified as the initial liability on which to focus (C_{max} = 320 nM and AUC_{0-5h} = 972 h nM).[153]

A medicinal chemistry campaign began with replacement of the potentially metabolically labile 3,4-(methylenedioxy)aniline (R_6) and unsubstituted phenyl group (R_7) with 4-fluoro-substituted phenyl groups, resulting in a 4-fold increase in potency.[152] Variation of the glycine residue (R_3) with various amino acids revealed that the stereochemistry was not important and that the free amine was most favorable; therefore, glycine was chosen as the preferred side chain (**14**, Figure 12). In addition, α-methylalanine (**15**, Figure 12) was examined due to the potential enhancement of metabolic

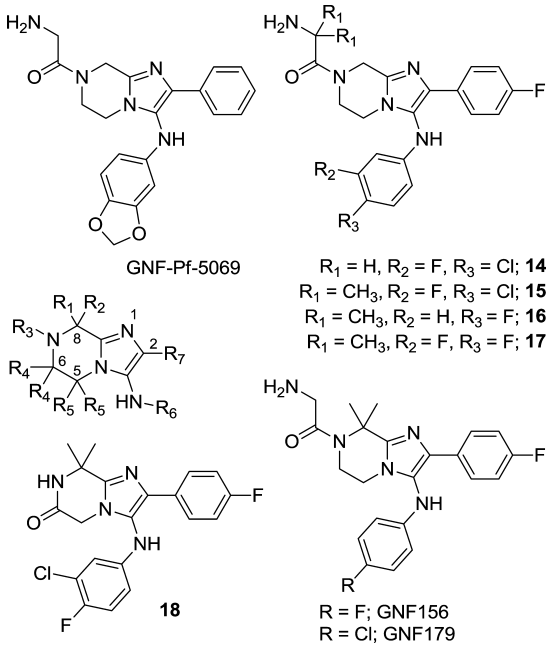

Figure 12. Development of GNF156/KAF156.

stability gained by blocking a theoretical metabolic hot spot without sacrificing activity. Various substitutions on the phenyl ring attached to the imidazole were poorly tolerated, and only small atoms (fluorine or hydrogen) in the *para* and *meta* positions provided high potency. Substituents on the aniline could be altered with more flexibility, with methyl, fluorine, and chlorine substitutions in the *para* and *meta* positions providing high-potency analogues. However, aliphatic rings and heterocyclic rings were not tolerated. Analogues from this series were also evaluated in an in vitro liver-stage assay, which revealed potent blockade of sporozoite infection of hepatocytes.[154]

In initial assessment of metabolic liabilities, the new potent analogues were found to possess good to moderate clearance in human and mouse microsomes, with a more rapid degradation observed in rat liver microsomes. In vivo PK data in mice revealed that the dimethylglycine analogues generally had low hepatic clearance and correspondingly higher exposure (AUC_{inf} = 6175 and 36 668 nM h for **14** and **15**, respectively) following oral dosing. Most of the analogues reduced parasitemia by >99% when administered as a single oral 100 mg/kg dose in the *P. berghei* mouse model and prolonged the mouse survival time for >10 days. The glycine analogues were found to be less efficacious, despite their better potencies (3D7 EC_{50} = 3 and 40 nM for **14** and **15**, respectively), which can be rationalized from their lower overall plasma exposures.

The two most efficacious analogues (**16** and **17**, Figure 12) were analyzed to establish their toxicology profile. Neither compound inhibited any tested CYP450 (IC_{50} values were greater than 9 μM for CYP1A2, CYP2C19, CYP2C9, CYP2D6, and CYP3A4) or possessed significant cytotoxicity (EC_{50} > 12 μM for 293T, Ba/F3, CHO, HEp2, HeLa, and Huh7). In addition, in dose-ranging studies in rats, no gross effects were found for **16** at doses up to 500 mg/kg. Compound **17** was negative in the mini-Ames and micronucleus tests. One potential safety concern was moderately potent inhibition of the hERG channel (IC_{50} values of 6 and 5 μM for **16** and **17**, respectively).

Subsequent synthetic efforts were focused on exploring the chemistry around the piperazine ring to better balance potency, oral exposure, and hERG inhibition.[155] The initial focus was on the 8-position of the piperazine ring, which had been identified as an oxidation site leading to formation of inactive analogues in in vitro metabolic stability assays. The addition of a methyl group to the 8-position (either the (*S*)- or the (*R*)-conformation) resulted in a 10-fold loss in potency. An isopropyl group resulted in a greater reduction in potency. Introduction of a dimethyl group in the 8-position satisfied the goal of blocking the benzylic carbon from metabolic transformations and afforded an enhancement in antiplasmodial potency. On the basis of the success of the dimethyl substitution in the 8-position, the dimethyl group was shifted around the piperazine ring to both the 5- and 6-positions, with both alterations providing significantly less potent analogues. The 8,8-dimethyl substitution was thus deemed the optimal modification to the piperazine core. The minimal structure for activity was then re-evaluated, and it was determined that, for analogues in which the amino acid side chain was removed (R_3 = H), and where both the side chain was removed and a carbonyl was installed on the carbon at the 6-position to form the lactam (**18**, Figure 12), the 8,8-dimethyl substitutions provided suitably active compounds.

The pharmacokinetic properties of the new analogues were evaluated, and it was determined that the removal of the amino acid side chain (R_3 = H) caused significant improvements to permeability but negatively affected metabolic stability.[155] Overall, the permeability and metabolic stability did not improve with the introduction of the 8,8-dimethyl substitution despite the metabolism occurring at the 8-position of the piperazine. On the other hand, the 8,8-dimethyl did provide an advantage in that the hERG channel inhibition was reduced by at least 2−3-fold for most analogues. Snapshot PK analysis[153] showed a low to moderate clearance for the 8,8-dimethyl analogues, representing a significant improvement over the corresponding unsubstituted analogues.[155] The lactam analogue **18** exhibited the highest oral AUC values (2097 h nM from 0 to 5 h) and lowest intrinsic clearance of all analogues tested. Subsequent studies focused on **18**.

Efficacy studies in the *P. berghei* mouse model revealed the compound provided >99% reduction in parasitemia at a low dose (1 × 30 mg/kg) but only a modest extension of survival (≥15 days) without producing a complete cure. Examination of potency in vivo of other analogues revealed a ∼10-fold increase in potency with the inclusion of the glycine substitution at R_3 (ED_{99} = 2.2 mg/kg for GNF156) and indicated that the unsubstituted analogues (R_3 = H) were inferior in terms of both parasite reduction and survival in mice despite the superior oral exposure. The late lead GNF156 had poor oral exposure in rats but superior efficacy in mouse models of malaria. It was found to exhibit a 7-fold increase in AUC when the dose was escalated from 10 to 30 mg/kg and a 55-fold increase in AUC and a 3-fold increase in bioavailability when the dose was increased to 100 mg/kg.

As with previous analogues, GNF156 did not inhibit CYP450 isoforms (IC_{50} values were greater than 6 μM for CYP1A2, CYP2C19, CYP2C9, CYP2D6, and CYP3A4) and had low cytotoxicity (CC_{50} values for 293T, Ba/F3, CHO, HEp2, HeLa, and Huh7 were >12 μM). In addition, since the efficacious plasma C_{max} in the mouse was low, the risk of cardiotoxicity was deemed minimal as the hERG channel inhibitory activity was fairly weak (IC_{50} = 13.4 μM). GNF156 is currently in phase II

dx.doi.org/10.1021/cr500543f | *Chem. Rev.* 2014, 114, 11221−11241

clinical trials with adult patients with acute, uncomplicated *P. falciparum* or *P. vivax* malaria monoinfection (ClinicalTrials.gov identifier NCT01753323).

The activity observed for the liver stage was followed up with in vivo studies aimed at evaluating the causal prophylactic activity of GNF179.[154] GNF179 showed a liver C_{max} of 55 μM following a 15 mg/kg dose and 193 μM following a 100 mg/kg dose, with all other PK properties considered good. Following treatment with a single oral dose of 15 mg/kg, GNF179 was found to be fully protective against an infectious *P. berghei* sporozoite challenge, suggesting causal prophylactic activity.

The mechanism of action of imidazolopiperazines was also investigated as it was not believed to overlap with that of known antimalarials due to the lack of cross-resistance with drug-resistant mutants. *P. falciparum* Dd2 and 3D7 strains were exposed to three imidazolopiperazine analogues at constant and increasing drug concentrations until resistant mutants appeared. The mutants were subsequently sequenced, and it was revealed that a single gene was mutated in all resistant strains, *PF*C0970w, named the *P. falciparum* cyclic amine resistance locus (*Pf*carl).[154] *Pf*carl encodes a transmembrane protein with conserved homologues across almost all eukaryotic genera believed to play a role in protein folding within the endoplasmic reticulum.

3.4. 3,5-Diaryl-2-aminopyridine MMV390048

A high-throughput screen of a 37 000-membered BioFocus kinase library identified 442 compounds that significantly inhibited proliferation of *P. falciparum* asexual stages at 2 μM.[156] Follow-up of the active compounds from the screening effort led to the identification of eight compounds within the 3,5-diaryl-2-aminopyridine chemotype that showed >80% inhibition at 2 μM.[157] Other examples of this chemotype were also reported in the GSK Tres Cantos Antimalarial Set (TCAMS)[158] and in the Novartis (GNF) Malaria Screening data set.[141a,154] SAR analysis of the hit compounds revealed that analogues with a (methylsulfonyl)phenyl group at the 5-position (**19**, Figure 13) of the aminopyridine core provided the best potencies. Compound **19** was resynthesized and retested and found to be highly potent (IC_{50} = 49 nM, K1 and NF54). It was selected as a lead compound for further development.

Investigation of the metabolic stability in human liver microsomes revealed moderate stability (E_H = 0.48), predicting rapid clearance in vivo.[157] On the basis of the prediction that the 2-methoxyphenyl moiety at the 3-position of the aminopyridine core was the source of the metabolic liability, a limited analogue set was constructed to lessen metabolism. This effort resulted in the identification of an equipotent analogue (**20**, IC_{50} = 51 nM, K1 and NF54) exhibiting more favorable metabolic stability (E_H = 0.26). Subsequent structure–activity studies found *para* and *meta* substitutions on the 3-position aryl group to be well tolerated, whereas *ortho* substitutions caused a significant reduction in potency. It was also determined that replacement of the benzene ring with a pyridine did not negatively affect activity. From this set of analogues, the most promising compounds in terms of antiplasmodial potency were evaluated for their physiochemical properties and in vitro metabolic stabilities in human liver microsomes. Partition coefficient values[159] were generally moderate (log $D_{7.4}$ = 1.5–3.6), kinetic solubility[160] ranged from poor to moderate, and protein binding[161] varied broadly (74.4–96.9%), generally

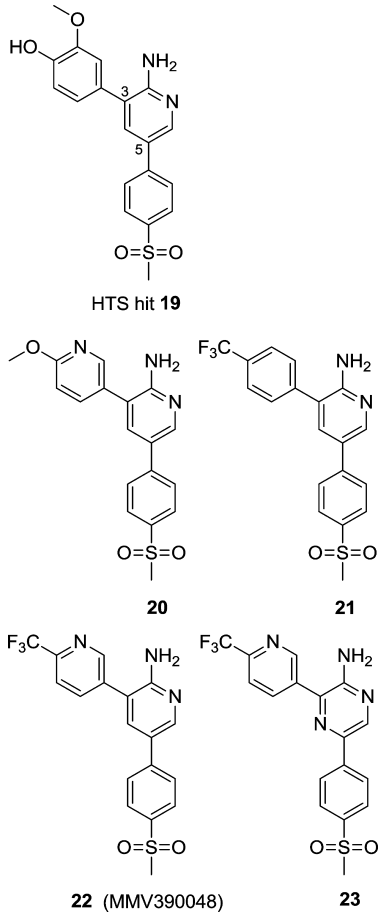

Figure 13. Development of MMV390048.

correlating to log *D*. The analogues were stable in mouse, rat, and human liver microsomes.

Analogues that showed improved metabolic stability while retaining antiplasmodial potency were evaluated in vivo in *P. berghei* infected mice.[157] Several compounds gave >99% reduction in parasitemia after oral administration (4 × 50 mg/kg doses); two were curative (**20** and **22**, Figure 13). A single adverse event was reported for compound **21**, impaired coordination in the animals following the administration of the third dose, although high reduction of parasitemia (97.3% and 98%) was observed at single doses of 30 and 10 mg/kg, respectively. Furthermore, compound **22** was found to be completely curative after a single dose of either 30 or 100 mg/kg with ED_{50} and ED_{90} values of 1 and 2 mg/kg, respectively. Evaluation of the PK profiles for the efficacious analogues following administration of 5 mg/kg intravenously and 5 or 20 mg/kg orally to rats revealed good oral bioavailability for **20** (~83%) with a half-life of ~8 h. Analogue **21** was found to have lower bioavailability (26%), while **22** showed good bioavailability (51% at 20 mg/kg), a favorable half-life (7–8 h), low clearance (6.5 mL/min/kg), and a moderate volume of distribution (2.7 L/kg). Toxicological analysis of **20** and **22** showed low potential for inhibition of the five major CYP450 isoforms, no genotoxicity risk in the Ames assay, and moderate effects on hERG (**20**, IC_{50} = 5.5 μM; **22**, IC_{50} = 4.7–11 μM). The hERG activity was followed up with an in vitro analysis of **22** in a rabbit ventricular wedge assay that displayed no change in QT interval (QT), the interval between the start of the Q wave and the end of the T wave on ECG; TP-e interval (TP-e),

dx.doi.org/10.1021/cr500543f | *Chem. Rev.* 2014, 114, 11221–11241

the interval between the peak and the end of the T wave on ECG; and QRS complex (QRS) at a concentration of 2 μM, suggesting the hERG signal is likely to have a minimal impact in vivo.

To address the potential hERG liability, a small number of new analogues were synthesized combining the optimized *p*-(trifluoromethyl)aryl substituent in the 3-position (**20** and **22**) with a variety of different arenes in the 5-position.[162] Substituents in the *meta* and *ortho* positions were found to be strongly disfavored, as were lipophilic electron-withdrawing groups ($-OCF_3$ or $-CF_3$) in the *para* position. Potent activity was achieved with polar, electron-withdrawing groups, including N-substituted sulfonamides and primary, secondary, or tertiary carboxamides. Improvement in hERG activity was achieved with this set of analogues compared to compounds **20** and **22**, but when the hERG-optimized analogues were evaluated in vivo against *P. berghei*, they were found to be less efficacious at lower doses and none were able to produce a cure.

The SAR of 3,5-diarylaminopyridines was explored further through the synthesis and evaluation of analogues with modifications around the central 2-aminopyridine core.[163] It was determined that the primary 2-amino group is essential for antiplasmodial activity, with replacement (with H, OH, I, or CF_3) or substitution to form the methylamine causing a significant loss of potency. With the requisite 2-amino group fixed, the pyridine core was modified, revealing that replacement with a phenyl, pyridazine, or thienopyridine group led to a loss of activity, as did moving the position of the pyridine nitrogen. However, a more potent analogue was found when the pyridine was replaced with a pyrazine, yielding compound **23** (NF54 IC_{50} = 10 nM). In general, 2-aminopyrazine analogues provided slightly better antiplasmodial potencies than the corresponding 2-aminopyridine analogues. However, these analogues possessed poor to moderate kinetic solubility, moderate partition coefficients (log *D* between 1.7 and 3.2), and good metabolic stability in human liver microsomes. Evaluation of the efficacy of **23** in *P. berghei* infected mice showed potent activity at a single oral dose of 3 mg/kg and multiple oral doses of 4 × 1 mg/kg, with 99.4% and 99.9% reduction in parasitemia, respectively. Compound **23** was also found to be completely curative at an oral dose of 4 × 10 mg/kg (MSD > 30 days).[163] Ultimately, from the series of 3,5-diarylaminopyridines synthesized, analogue **22** (MMV390048) was chosen as a clinical candidate, and a phase I study is currently under way (www.mmv.org).

4. FINAL REMARKS

Over the past decade, substantial progress has been made toward the identification of new chemical entities geared for the fight against malaria. Modifications of flawed drugs through modern insight, re-engineering molecules on the basis of proven pharmacophores, and capitalizing on the biological niches of the parasite have proven to be successful strategies in malaria drug discovery. However, the power and effectiveness of the generation of high-quality lead compounds available through utilization of a high-throughput phenotypic screening approach is difficult to dispute. In such efforts, active compounds simply select for growth inhibition without any biological bias based on mechanism of action. This allows for the generation of many lead compound series that can subsequently be prioritized on the basis of criteria that are most pertinent for a given circumstance. While HTS has become the major tool for hit generation, fundamental research will always be required to elucidate the biological foundation for mechanism.

AUTHOR INFORMATION

Corresponding Author

*E-mail: kip.guy@stjude.org.

Notes

The authors declare no competing financial interest.

Biographies

David S. Barnett was born in Colorado and attended the University of Colorado, Boulder, where he received his B.A. in biochemistry and graduated magna cum laude for his contribution to the bacterial chemotaxis research conducted in the Falke laboratory. He then traveled to Boston University for his Ph.D. research, where he developed organic, asymmetric boronate exchange reaction methodologies in the Schaus laboratory using chiral, organic diol catalysts to synthesize homoallyic, homopropargylic, and α-allenic alcohols in high yield and enantiopurity. David is currently a postdoctoral fellow at St. Jude Children's Research Hospital, where he hopes to contribute to Kip Guy's mission to deliver novel chemical scaffolds to the fight against malaria.

R. Kiplin Guy received his B.A. in chemistry from Reed College and his Ph.D. in organic chemistry from The Scripps Research Institute on the basis of his work on the total synthesis of paclitaxel in the Nicolaou laboratory. After completion of a postdoctoral fellowship with Brown and Goldstein at UT Southwestern, he joined the faculty at the University of California, San Francisco, where he rose to the rank of Professor. In 2005 he moved to St. Jude to chair the new Department of Chemical Biology and Therapeutics. His group is focused on medicinal chemistry for catastrophic pediatric illnesses.

REFERENCES

(1) World Health Organization. *World Malaria Report*; Geneva, Switzerland, 2012.

(2) (a) Noedl, H.; Se, Y.; Schaecher, K.; Smith, B. L.; Socheat, D.; Fukuda, M. M. *N. Engl. J. Med.* **2008**, *359*, 2619. (b) Dondorp, A. M.; Nosten, F.; Yi, P.; Das, D.; Phyo, A. P.; Tarning, J.; Lwin, K. M.; Ariey, F.; Hanpithakpong, W.; Lee, S. J.; Ringwald, P.; Silamut, K.; Imwong, M.; Chotivanich, K.; Lim, P.; Herdman, T.; An, S. S.; Yeung, S.; Singhasivanon, P.; Day, N. P.; Lindegardh, N.; Socheat, D.; White, N. J. *N. Engl. J. Med.* **2009**, *361*, 455.

(3) Leroy, D.; Campo, B.; Ding, X. C.; Burrows, J. N.; Cherbuin, S. *Trends Parasitol.* **2014**, *30*, 478.

(4) Smithson, D. C.; Guiguemde, W. A.; Guy, R. K. In *Burger's Medicinal Chemistry, Drug Discovery and Development, Vol. 7: Antiinfectives*; Abraham, D. J., Rotella, D. P., Eds.; Wiley: Hoboken, NJ, 2010; pp 603−712.

(5) (a) Biamonte, M. A.; Wanner, J.; Le Roch, K. G. *Bioorg. Med. Chem. Lett.* **2013**, *23*, 2829. (b) Schrader, F. C.; Barho, M.; Steiner, I.; Ortmann, R.; Schlitzer, M. *Int. J. Med. Microbiol.* **2012**, *302*, 165. (c) Anthony, M. P.; Burrows, J. N.; Duparc, S.; Moehrle, J. J.; Wells, T. N. *Malar. J.* **2012**, *11*, 316. (d) Jefford, C. W. *Curr. Top. Med. Chem.* **2012**, *12*, 373. (e) Tilley, L.; Charman, S. A.; Vennerstrom, J. L. In *Neglected Diseases and Drug Discovery*; Palmer, M. J., Wells, T. N. C., Eds.; Royal Society of Chemistry: Cambridge, U.K., 2012; pp 33−64. (f) Schlitzer, M. *ChemMedChem* **2007**, *2*, 944.

(6) (a) Wellems, T. E.; Plowe, C. V. *J. Infect. Dis.* **2001**, *184*, 770. (b) Hastings, I. M.; Bray, P. G.; Ward, S. A. *Science* **2002**, *298*, 74.

(7) Dive, D.; Biot, C. *ChemMedChem* **2008**, *3*, 383.

(8) Marcsisin, S. R.; Sousa, J. C.; Reichard, G. A.; Caridha, D.; Zeng, Q.; Roncal, N.; McNulty, R.; Careagabarja, J.; Sciotti, R. J.; Bennett, J. W.; Zottig, V. E.; Deye, G.; Li, Q.; Read, L.; Hickman, M.; Dhammika Nanayakkara, N. P.; Walker, L. A.; Smith, B.; Melendez, V.; Pybus, B. S. *Malar. J.* **2014**, *13*, 2.

(9) De, D.; Krogstad, F. M.; Cogswell, F. B.; Krogstad, D. J. *Am. J. Trop. Med. Hyg.* **1996**, *55*, 579.

(10) Berliner, R. W.; Earle, D. P.; Taggart, J. V.; Zubrod, C. G.; Welch, W. J.; Conan, N. J.; Bauman, E.; Scudder, S. T.; Shannon, J. A. *J. Clin. Invest.* **1948**, *27*, 98.

(11) Mzayek, F.; Deng, H.; Mather, F. J.; Wasilevich, E. C.; Liu, H.; Hadi, C. M.; Chansolme, D. H.; Murphy, H. A.; Melek, B. H.; Tenaglia, A. N.; Mushatt, D. M.; Dreisbach, A. W.; Lertora, J. J.; Krogstad, D. J. *PLoS Clin. Trials* **2007**, *2*, e6.

(12) Riccio, E. S.; Lee, P. S.; Winegar, R. A.; Krogstad, D. J.; De, D.; Mirsalis, J. C. *Environ. Mol. Mutagen.* **2001**, *38*, 69.

(13) Ramanathan-Girish, S.; Catz, P.; Creek, M. R.; Wu, B.; Thomas, D.; Krogstad, D. J.; De, D.; Mirsalis, J. C.; Green, C. E. *Int. J. Toxicol.* **2004**, *23*, 179.

(14) O'Neill, P. M.; Ward, S. A.; Berry, N. G.; Jeyadevan, J. P.; Biagini, G. A.; Asadollaly, E.; Park, B. K.; Bray, P. G. *Curr. Top. Med. Chem.* **2006**, *6*, 479.

(15) Watkins, W. M.; Sixsmith, D. G.; Spencer, H. C.; Boriga, D. A.; Kariuki, D. M.; Kipingor, T.; Koech, D. K. *Lancet* **1984**, *1*, 357.

(16) (a) Lind, D. E.; Levi, J. A.; Vincent, P. C. *Br. Med. J.* **1973**, *1*, 458. (b) Neftel, K. A.; Woodtly, W.; Schmid, M.; Frick, P. G.; Fehr, J. *Br. Med. J.* **1986**, *292*, 721. (c) Hatton, C. S.; Peto, T. E.; Bunch, C.; Pasvol, G.; Russell, S. J.; Singer, C. R.; Edwards, G.; Winstanley, P. *Lancet* **1986**, *1*, 411.

(17) Harrison, A. C.; Kitteringham, N. R.; Clarke, J. B.; Park, B. K. *Biochem. Pharmacol.* **1992**, *43*, 1421.

(18) Maggs, J. L.; Tingle, M. D.; Kitteringham, N. R.; Park, B. K. *Biochem. Pharmacol.* **1988**, *37*, 303.

(19) Johansson, T.; Jurva, U.; Gronberg, G.; Weidolf, L.; Masimirembwa, C. *Drug Metab. Dispos.* **2009**, *37*, 571.

(20) Tingle, M. D.; Jewell, H.; Maggs, J. L.; O'Neill, P. M.; Park, B. K. *Biochem. Pharmacol.* **1995**, *50*, 1113.

(21) O'Neill, P. M.; Mukhtar, A.; Stocks, P. A.; Randle, L. E.; Hindley, S.; Ward, S. A.; Storr, R. C.; Bickley, J. F.; O'Neil, I. A.; Maggs, J. L.; Hughes, R. H.; Winstanley, P. A.; Bray, P. G.; Park, B. K. *J. Med. Chem.* **2003**, *46*, 4933.

(22) (a) Barnard, S.; Kelly, D. F.; Storr, R. C.; Park, B. K. *Biochem. Pharmacol.* **1993**, *46*, 841. (b) Barnard, S.; Storr, R. C.; O'Neill, P. M.; Park, B. K. *J. Pharm. Pharmacol.* **1993**, *45*, 736.

(23) O'Neill, P. M.; Harrison, A. C.; Storr, R. C.; Hawley, S. R.; Ward, S. A.; Park, B. K. *J. Med. Chem.* **1994**, *37*, 1362.

(24) O'Neill, P. M.; Shone, A. E.; Stanford, D.; Nixon, G.; Asadollahy, E.; Park, B. K.; Maggs, J. L.; Roberts, P.; Stocks, P. A.; Biagini, G.; Bray, P. G.; Davies, J.; Berry, N.; Hall, C.; Rimmer, K.; Winstanley, P. A.; Hindley, S.; Bambal, R. B.; Davis, C. B.; Bates, M.; Gresham, S. L.; Brigandi, R. A.; Gomez-de-Las-Heras, F. M.; Gargallo, D. V.; Parapini, S.; Vivas, L.; Lander, H.; Taramelli, D.; Ward, S. A. *J. Med. Chem.* **2009**, *52*, 1828.

(25) Peters, W.; Robinson, B. L. In *Handbook of Animal Models of Infection: Experimental Models in Antimicrobial Chemotherapy*; Zak, O., Sande, M. A., Eds.; Academic Press: San Diego, CA, 1999; pp 757−773.

(26) Wennerholm, A.; Nordmark, A.; Pihlsgard, M.; Mahindi, M.; Bertilsson, L.; Gustafsson, L. L. *Eur. J. Clin. Pharmacol.* **2006**, *62*, 539.

(27) O'Neill, P. M.; Park, B. K.; Shone, A. E.; Maggs, J. L.; Roberts, P.; Stocks, P. A.; Biagini, G. A.; Bray, P. G.; Gibbons, P.; Berry, N.; Winstanley, P. A.; Mukhtar, A.; Bonar-Law, R.; Hindley, S.; Bambal, R. B.; Davis, C. B.; Bates, M.; Hart, T. K.; Gresham, S. L.; Lawrence, R. M.; Brigandi, R. A.; Gomez-delas-Heras, F. M.; Gargallo, D. V.; Ward, S. A. *J. Med. Chem.* **2009**, *52*, 1408.

(28) Rwagacondo, C. E.; Karema, C.; Mugisha, V.; Erhart, A.; Dujardin, J. C.; Van Overmeir, C.; Ringwald, P.; D'Alessandro, U. *Trop. Med. Int. Health* **2004**, *9*, 1091.

(29) Lawrence, R. M.; Dennis, K. C.; O'Neill, P. M.; Hahn, D. U.; Roeder, M.; Struppe, C. *Org. Process Res. Dev.* **2008**, *12*, 294.

(30) Sullivan, D. J. *Int. J. Parasitol.* **2002**, *32*, 1645.

(31) Parapini, S.; Basilico, N.; Pasini, E.; Egan, T. J.; Olliaro, P.; Taramelli, D.; Monti, D. *Exp. Parasitol.* **2000**, *96*, 249.

(32) Moreau, S.; Perly, B.; Biguet, J. *Biochimie* **1982**, *64*, 1015.

(33) Davis, C. B.; Bambal, R.; Moorthy, G. S.; Hugger, E.; Xiang, H.; Park, B. K.; Shone, A. E.; O'Neill, P. M.; Ward, S. A. *J. Pharm. Sci.* **2009**, *98*, 362.

(34) Bustos, M. D.; Gay, F.; Diquet, B.; Thomare, P.; Warot, D. *Trop. Med. Parasitol.* **1994**, *45*, 83.

(35) Kindermans, J. M.; Pilloy, J.; Olliaro, P.; Gomes, M. *Malar. J.* **2007**, *6*, 125.

(36) Paddon, C. J.; Westfall, P. J.; Pitera, D. J.; Benjamin, K.; Fisher, K.; McPhee, D.; Leavell, M. D.; Tai, A.; Main, A.; Eng, D.; Polichuk, D. R.; Teoh, K. H.; Reed, D. W.; Treynor, T.; Lenihan, J.; Jiang, H.; Fleck, M.; Bajad, S.; Dang, G.; Dengrove, D.; Diola, D.; Dorin, G.; Ellens, K. W.; Fickes, S.; Galazzo, J.; Gaucher, S. P.; Geistlinger, T.; Henry, R.; Hepp, M.; Horning, T.; Iqbal, T.; Kizer, L.; Lieu, B.; Melis, D.; Moss, N.; Regentin, R.; Secrest, S.; Tsuruta, H.; Vazquez, R.; Westblade, L. F.; Xu, L.; Yu, M.; Zhang, Y.; Zhao, L.; Lievense, J.; Covello, P. S.; Keasling, J. D.; Reiling, K. K.; Renninger, N. S.; Newman, J. D. *Nature* **2013**, *496*, 528.

(37) (a) Levesque, F.; Seeberger, P. H. *Angew. Chem., Int. Ed.* **2012**, *51*, 1706. (b) Kopetzki, D.; Levesque, F.; Seeberger, P. H. *Chemistry* **2013**, *19*, 5450.

(38) Gilmore, K.; Kopetzki, D.; Lee, J. W.; Horvath, Z.; McQuade, D. T.; Seidel-Morgenstern, A.; Seeberger, P. H. *Chem. Commun.* **2014**, *50*, 12652.

(39) White, N. J. *Science* **2008**, *320*, 330.

(40) (a) White, N. J. *Antimicrob. Agents Chemother.* **1997**, *41*, 1413. (b) Li, Q. G.; Peggins, J. O.; Fleckenstein, L. L.; Masonic, K.; Heiffer, M. H.; Brewer, T. G. *J. Pharm. Pharmacol.* **1998**, *50*, 173. (c) Navaratnam, V.; Mansor, S. M.; Sit, N. W.; Grace, J.; Li, Q.; Olliaro, P. *Clin. Pharmacokinet.* **2000**, *39*, 255.

(41) Haynes, R. K.; Fugmann, B.; Stetter, J.; Rieckmann, K.; Heilmann, H. D.; Chan, H. W.; Cheung, M. K.; Lam, W. L.; Wong, H. N.; Croft, S. L.; Vivas, L.; Rattray, L.; Stewart, L.; Peters, W.; Robinson, B. L.; Edstein, M. D.; Kotecka, B.; Kyle, D. E.; Beckermann, B.; Gerisch, M.; Radtke, M.; Schmuck, G.; Steinke, W.; Wollborn, U.; Schmeer, K.; Romer, A. *Angew. Chem., Int. Ed.* **2006**, *45*, 2082.

(42) (a) Wesche, D. L.; DeCoster, M. A.; Tortella, F. C.; Brewer, T. G. *Antimicrob. Agents Chemother.* **1994**, *38*, 1813. (b) Fishwick, J.; McLean, W. G.; Edwards, G.; Ward, S. A. *Chem.-Biol. Interact.* **1995**, *96*, 263. (c) McLean, W. G.; Ward, S. A. *Med. Trop. (Marseille)* **1998**, *58*, 28.
(43) (a) Brewer, T. G.; Grate, S. J.; Peggins, J. O.; Weina, P. J.; Petras, J. M.; Levine, B. S.; Heiffer, M. H.; Schuster, B. G. *Am. J. Trop. Med. Hyg.* **1994**, *51*, 251. (b) Kamchonwongpaisan, S.; McKeever, P.; Hossler, P.; Ziffer, H.; Meshnick, S. R. *Am. J. Trop. Med. Hyg.* **1997**, *56*, 7. (c) Nontprasert, A.; Nosten-Bertrand, M.; Pukrittayakamee, S.; Vanijanonta, S.; Angus, B. J.; White, N. J. *Am. J. Trop. Med. Hyg.* **1998**, *59*, 519.
(44) (a) Bhattacharjee, A. K.; Karle, J. M. *Chem. Res. Toxicol.* **1999**, *12*, 422. (b) Haynes, R. K. *Curr. Opin. Infect. Dis.* **2001**, *14*, 719.
(45) Schmuck, G.; Ahr, H. J.; Schluter, G. *Vitro Mol. Toxicol.* **2000**, *13*, 37.
(46) (a) Schmuck, G.; Roehrdanz, E.; Haynes, R. K.; Kahl, R. *Antimicrob. Agents Chemother.* **2002**, *46*, 821. (b) Schmuck, G.; Haynes, R. K. *Neurotoxic. Res.* **2000**, *2*, 37.
(47) Eckstein-Ludwig, U.; Webb, R. J.; Van Goethem, I. D.; East, J. M.; Lee, A. G.; Kimura, M.; O'Neill, P. M.; Bray, P. G.; Ward, S. A.; Krishna, S. *Nature* **2003**, *424*, 957.
(48) Uhlemann, A. C.; Cameron, A.; Eckstein-Ludwig, U.; Fischbarg, J.; Iserovich, P.; Zuniga, F. A.; East, M.; Lee, A.; Brady, L.; Haynes, R. K.; Krishna, S. *Nat. Struct. Mol. Biol.* **2005**, *12*, 628.
(49) Nagelschmitz, J.; Voith, B.; Wensing, G.; Roemer, A.; Fugmann, B.; Haynes, R. K.; Kotecka, B. M.; Rieckmann, K. H.; Edstein, M. D. *Antimicrob. Agents Chemother.* **2008**, *52*, 3085.
(50) (a) Na-Bangchang, K.; Congpoung, K.; Ubalee, R.; Thanavibul, A.; Tan-anya, P.; Karbwang, J. *Southeast Asian J. Trop. Med. Public Health.* **1997**, *28*, 731. (b) Teja-Isavadharm, P.; Nosten, F.; Kyle, D. E.; Luxemburger, C.; Ter Kuile, F.; Peggins, J. O.; Brewer, T. G.; White, N. J. *Br. J. Clin. Pharmacol.* **1996**, *42*, 599.
(51) Tang, Y.; Dong, Y.; Vennerstrom, J. L. *Med. Res. Rev.* **2004**, *24*, 425.
(52) Vennerstrom, J. L.; Arbe-Barnes, S.; Brun, R.; Charman, S. A.; Chiu, F. C. K.; Chollet, J.; Dong, Y. X.; Dorn, A.; Hunziker, D.; Matile, H.; McIntosh, K.; Padmanilayam, M.; Tomas, J. S.; Scheurer, C.; Scorneaux, B.; Tang, Y. Q.; Urwyler, H.; Wittlin, S.; Charman, W. N. *Nature* **2004**, *430*, 900.
(53) Griesbaum, K.; Liu, X.; Kassiaris, A.; Scherer, M. *Liebigs Ann.* **1997**, *1997*, 1381.
(54) Kaiser, M.; Wittlin, S.; Nehrbass-Stuedli, A.; Dong, Y.; Wang, X.; Hemphill, A.; Matile, H.; Brun, R.; Vennerstrom, J. L. *Antimicrob. Agents Chemother.* **2007**, *51*, 2991.
(55) Dong, Y.; Chollet, J.; Matile, H.; Charman, S. A.; Chiu, F. C.; Charman, W. N.; Scorneaux, B.; Urwyler, H.; Santo Tomas, J.; Scheurer, C.; Snyder, C.; Dorn, A.; Wang, X.; Karle, J. M.; Tang, Y.; Wittlin, S.; Brun, R.; Vennerstrom, J. L. *J. Med. Chem.* **2005**, *48*, 4953.
(56) Vennerstrom, J. L.; Dong, Y.; Chollet, J.; Matile, H. US 20026486199.
(57) Hofer, S.; Brun, R.; Maerki, S.; Matile, H.; Scheurer, C.; Wittlin, S. *J. Antimicrob. Chemother.* **2008**, *62*, 1061.
(58) Maerki, S.; Brun, R.; Charman, S. A.; Dorn, A.; Matile, H.; Wittlin, S. *J. Antimicrob. Chemother.* **2006**, *58*, 52.
(59) Vyas, N.; Avery, B. A.; Avery, M. A.; Wyandt, C. M. *Antimicrob. Agents Chemother.* **2002**, *46*, 105.
(60) Gordi, T.; Lepist, E. I. *Toxicol. Lett.* **2004**, *147*, 99.
(61) Olliaro, P.; Wells, T. N. *Clin. Pharmacol. Ther.* **2009**, *85*, 584.
(62) Valecha, N.; Looareesuwan, S.; Martensson, A.; Abdulla, S. M.; Krudsood, S.; Tangpukdee, N.; Mohanty, S.; Mishra, S. K.; Tyagi, P. K.; Sharma, S. K.; Moehrle, J.; Gautam, A.; Roy, A.; Paliwal, J. K.; Kothari, M.; Saha, N.; Dash, A. P.; Bjorkman, A. *Clin. Infect. Dis.* **2010**, *51*, 684.
(63) Rathi, A. Ranbaxy launches new anti-malarial Synriam, 2012. http://www.rsc.org/chemistryworld/2012/05/ranbaxy-launches-new-anti-malarial-synriam (accessed Oct 12, 2014).
(64) Zhou, L.; Alker, A.; Ruf, A.; Wang, X.; Chiu, F. C.; Morizzi, J.; Charman, S. A.; Charman, W. N.; Scheurer, C.; Wittlin, S.; Dong, Y.; Hunziker, D.; Vennerstrom, J. L. *Bioorg. Med. Chem. Lett.* **2008**, *18*, 1555.
(65) Charman, S. A.; Arbe-Barnes, S.; Bathurst, I. C.; Brun, R.; Campbell, M.; Charman, W. N.; Chiu, F. C.; Chollet, J.; Craft, J. C.; Creek, D. J.; Dong, Y.; Matile, H.; Maurer, M.; Morizzi, J.; Nguyen, T.; Papastogiannidis, P.; Scheurer, C.; Shackleford, D. M.; Sriraghavan, K.; Stingelin, L.; Tang, Y.; Urwyler, H.; Wang, X.; White, K. L.; Wittlin, S.; Zhou, L.; Vennerstrom, J. L. *Proc. Natl. Acad. Sci. U.S.A.* **2011**, *108*, 4400.
(66) (a) Balani, S. K.; Zhu, T.; Yang, T. J.; Liu, Z.; He, B.; Lee, F. W. *Drug Metab. Dispos.* **2002**, *30*, 1059. (b) Strelevitz, T. J.; Foti, R. S.; Fisher, M. B. *J. Pharm. Sci.* **2006**, *95*, 1334.
(67) (a) Fugi, M. A.; Wittlin, S.; Dong, Y.; Vennerstrom, J. L. *Antimicrob. Agents Chemother.* **2010**, *54*, 1042. (b) Creek, D. J.; Charman, W. N.; Chiu, F. C.; Prankerd, R. J.; Dong, Y.; Vennerstrom, J. L.; Charman, S. A. *Antimicrob. Agents Chemother.* **2008**, *52*, 1291. (c) Wang, X.; Dong, Y.; Wittlin, S.; Creek, D.; Chollet, J.; Charman, S. A.; Tomas, J. S.; Scheurer, C.; Snyder, C.; Vennerstrom, J. L. *J. Med. Chem.* **2007**, *50*, 5840.
(68) Creek, D. J.; Charman, W. N.; Chiu, F. C.; Prankerd, R. J.; McCullough, K. J.; Dong, Y.; Vennerstrom, J. L.; Charman, S. A. *J. Pharm. Sci.* **2007**, *96*, 2945.
(69) Creek, D. J.; Chalmers, D. K.; Charman, W. N.; Duke, B. J. *J. Mol. Graphics Modell.* **2008**, *27*, 394.
(70) Moehrle, J. J.; Duparc, S.; Siethoff, C.; van Giersbergen, P. L.; Craft, J. C.; Arbe-Barnes, S.; Charman, S. A.; Gutierrez, M.; Wittlin, S.; Vennerstrom, J. L. *Br. J. Clin. Pharmacol.* **2013**, *75*, 524.
(71) Angyan, L. *Orv. Hetil.* **1991**, *132*, 899.
(72) O'Neill, P. M.; Amewu, R. K.; Nixon, G. L.; Bousejra ElGarah, F.; Mungthin, M.; Chadwick, J.; Shone, A. E.; Vivas, L.; Lander, H.; Barton, V.; Muangnoicharoen, S.; Bray, P. G.; Davies, J.; Park, B. K.; Wittlin, S.; Brun, R.; Preschel, M.; Zhang, K.; Ward, S. A. *Angew. Chem., Int. Ed.* **2010**, *49*, 5693.
(73) Opsenica, I.; Opsenica, D.; Smith, K. S.; Milhous, W. K.; Solaja, B. A. *J. Med. Chem.* **2008**, *51*, 2261.
(74) (a) Amewu, R.; Stachulski, A. V.; Ward, S. A.; Berry, N. G.; Bray, P. G.; Davies, J.; Labat, G.; Vivas, L.; O'Neill, P. M. *Org. Biomol. Chem.* **2006**, *4*, 4431. (b) Ellis, G. L.; Amewu, R.; Sabbani, S.; Stocks, P. A.; Shone, A.; Stanford, D.; Gibbons, P.; Davies, J.; Vivas, L.; Charnaud, S.; Bongard, E.; Hall, C.; Rimmer, K.; Lozanom, S.; Jesus, M.; Gargallo, D.; Ward, S. A.; O'Neill, P. M. *J. Med. Chem.* **2008**, *51*, 2170.
(75) Peters, W.; Fleck, S. L.; Robinson, B. L.; Stewart, L. B.; Jefford, C. W. *Ann. Trop. Med. Parasitol.* **2002**, *96*, 559.
(76) Vial, H.; Ancelin, M. L. In *Malaria: Parasite Biology, Pathogenesis, and Protection*; Sherman, I. W., Ed.; ASM Press: Washington, DC, 1998; pp 159−175.
(77) (a) Ancelin, M. L.; Vial, H. J. *Biochim. Biophys. Acta, Lipids Lipid Metab.* **1989**, *1001*, 82. (b) Ancelin, M. L.; Parant, M.; Thuet, M. J.; Philippot, J. R.; Vial, H. J. *Biochem. J.* **1991**, *273*, 701.
(78) Ancelin, M. L.; Vial, H. J. *Antimicrob. Agents Chemother.* **1986**, *29*, 814.
(79) Ancelin, M. L.; Calas, M.; Bompart, J.; Cordina, G.; Martin, D.; Ben Bari, M.; Jei, T.; Druilhe, P.; Vial, H. J. *Blood* **1998**, *91*, 1426.
(80) Calas, M.; Cordina, G.; Bompart, J.; Ben Bari, M.; Jei, T.; Ancelin, M. L.; Vial, H. *J. Med. Chem.* **1997**, *40*, 3557.
(81) Calas, M.; Ancelin, M. L.; Cordina, G.; Portefaix, P.; Piquet, G.; Vidal-Sailhan, V.; Vial, H. *J. Med. Chem.* **2000**, *43*, 505.
(82) Ancelin, M. L.; Vialettes, F.; Vial, H. J. *Anal. Biochem.* **1991**, *199*, 203.
(83) Ancelin, M. L.; Calas, M.; Vidal-Sailhan, V.; Herbute, S.; Ringwald, P.; Vial, H. J. *Antimicrob. Agents Chemother.* **2003**, *47*, 2590.
(84) Wengelnik, K.; Vidal, V.; Ancelin, M. L.; Cathiard, A. M.; Morgat, J. L.; Kocken, C. H.; Calas, M.; Herrera, S.; Thomas, A. W.; Vial, H. J. *Science* **2002**, *295*, 1311.
(85) Ancelin, M. L.; Calas, M.; Bonhoure, A.; Herbute, S.; Vial, H. J. *Antimicrob. Agents Chemother.* **2003**, *47*, 2598.

(86) Hamze, A.; Rubi, E.; Arnal, P.; Boisbrun, M.; Carcel, C.; Salom-Roig, X.; Maynadier, M.; Wein, S.; Vial, H.; Calas, M. *J. Med. Chem.* **2005**, *48*, 3639.
(87) Vial, H. J.; Wein, S.; Farenc, C.; Kocken, C.; Nicolas, O.; Ancelin, M. L.; Bressolle, F.; Thomas, A.; Calas, M. *Proc. Natl. Acad. Sci. U.S.A.* **2004**, *101*, 15458.
(88) Peyrottes, S.; Caldarelli, S.; Wein, S.; Perigaud, C.; Pellet, A.; Vial, H. *Curr. Pharm. Des.* **2012**, *18*, 3454.
(89) Caldarelli, S. A.; Boisbrun, M.; Alarcon, K.; Hamze, A.; Ouattara, M.; Salom-Roig, X.; Maynadier, M.; Wein, S.; Peyrottes, S.; Pellet, A.; Calas, M.; Vial, H. *Bioorg. Med. Chem. Lett.* **2010**, *20*, 3953.
(90) Curd, F. H.; Davey, D. G.; Rose, F. L. *Ann. Trop. Med. Parasitol.* **1945**, *39*, 208.
(91) Carrington, H. C.; Crowther, A. F.; Davey, D. G.; Levi, A. A.; Rose, F. L. *Nature* **1951**, *168*, 1080.
(92) Falco, E. A.; Goodwin, L. G.; Hitchings, G. H.; Rollo, I. M.; Russell, P. B. *Br J. Pharmacol. Chemother.* **1951**, *6*, 185.
(93) (a) Foote, S. J.; Galatis, D.; Cowman, A. F. *Proc. Natl. Acad. Sci. U.S.A.* **1990**, *87*, 3014. (b) Peterson, D. S.; Milhous, W. K.; Wellems, T. E. *Proc. Natl. Acad. Sci. U.S.A.* **1990**, *87*, 3018. (c) Peterson, D. S.; Walliker, D.; Wellems, T. E. *Proc. Natl. Acad. Sci. U.S.A.* **1988**, *85*, 9114. (d) Sirawaraporn, W.; Sathitkul, T.; Sirawaraporn, R.; Yuthavong, Y.; Santi, D. V. *Proc. Natl. Acad. Sci. U.S.A.* **1997**, *94*, 1124. (e) Cowman, A. F.; Morry, M. J.; Biggs, B. A.; Cross, G. A.; Foote, S. J. *Proc. Natl. Acad. Sci. U.S.A.* **1988**, *85*, 9109.
(94) Burrows, J. N.; Chibale, K.; Wells, T. N. *Curr. Top. Med. Chem.* **2011**, *11*, 1226.
(95) (a) Yuvaniyama, J.; Chitnumsub, P.; Kamchonwongpaisan, S.; Vanichtanankul, J.; Sirawaraporn, W.; Taylor, P.; Walkinshaw, M. D.; Yuthavong, Y. *Nat. Struct. Biol.* **2003**, *10*, 357. (b) Yuthavong, Y.; Yuvaniyama, J.; Chitnumsub, P.; Vanichtanankul, J.; Chusacultanachai, S.; Tarnchompoo, B.; Vilaivan, T.; Kamchonwongpaisan, S. *Parasitology* **2005**, *130*, 249.
(96) Ferone, R. *J. Biol. Chem.* **1970**, *245*, 850.
(97) Rieckmann, K. H. *WHO Technol. Rep. Ser.* **1973**, *529*, 58.
(98) Yuthavong, Y.; Tarnchompoo, B.; Vilaivan, T.; Chitnumsub, P.; Kamchonwongpaisan, S.; Charman, S. A.; McLennan, D. N.; White, K. L.; Vivas, L.; Bongard, E.; Thongphanchang, C.; Taweechai, S.; Vanichtanankul, J.; Rattanajak, R.; Arwon, U.; Fantauzzi, P.; Yuvaniyama, J.; Charman, W. N.; Matthews, D. *Proc. Natl. Acad. Sci. U.S.A.* **2012**, *109*, 16823.
(99) Baker, B. R.; Jordaan, J. H. *J. Pharm. Sci.* **1965**, *54*, 1740.
(100) (a) Kuyper, L. F.; Roth, B.; Baccanari, D. P.; Ferone, R.; Beddell, C. R.; Champness, J. N.; Stammers, D. K.; Dann, J. G.; Norrington, F. E.; Baker, D. J.; Goodford, P. J. *J. Med. Chem.* **1985**, *28*, 303. (b) Rosowsky, A.; Forsch, R. A.; Queener, S. F. *J. Med. Chem.* **2002**, *45*, 233.
(101) Vaidya, A. B.; Mather, M. W. *Annu. Rev. Microbiol.* **2009**, *63*, 249.
(102) Fry, M.; Pudney, M. *Biochem. Pharmacol.* **1992**, *43*, 1545.
(103) Salzer, W.; Timmler, H.; Andersag, H. *Chem. Ber.* **1948**, *81*, 12.
(104) Kikuth, W.; Mudrowreichenow, L. *Z. Hyg. Infektionskrankh.* **1947**, *127*, 151.
(105) Winter, R.; Kelly, J. X.; Smilkstein, M. J.; Hinrichs, D.; Koop, D. R.; Riscoe, M. K. *Exp. Parasitol.* **2011**, *127*, 545.
(106) Cross, R. M.; Monastyrskyi, A.; Mutka, T. S.; Burrows, J. N.; Kyle, D. E.; Manetsch, R. *J. Med. Chem.* **2010**, *53*, 7076.
(107) (a) Markley, L. D.; Van Heertum, J. C.; Doorenbos, H. E. *J. Med. Chem.* **1972**, *15*, 1188. (b) Fry, M.; Williams, R. B. *Biochem. Pharmacol.* **1984**, *33*, 229.
(108) Yeates, C. L.; Batchelor, J. F.; Capon, E. C.; Cheesman, N. J.; Fry, M.; Hudson, A. T.; Pudney, M.; Trimming, H.; Woolven, J.; Bueno, J. M.; Chicharro, J.; Fernandez, E.; Fiandor, J. M.; Gargallo-Viola, D.; Gomez de las Heras, F.; Herreros, E.; Leon, M. L. *J. Med. Chem.* **2008**, *51*, 2845.
(109) Bueno, J. M.; Herreros, E.; Angulo-Barturen, I.; Ferrer, S.; Fiandor, J. M.; Gamo, F. J.; Gargallo-Viola, D.; Derimanov, G. *Future Med. Chem.* **2012**, *4*, 2311.
(110) Xiang, H.; McSurdy-Freed, J.; Moorthy, G. S.; Hugger, E.; Bambal, R.; Han, C.; Ferrer, S.; Gargallo, D.; Davis, C. B. *J. Pharm. Sci.* **2006**, *95*, 2657.
(111) Bueno, J. M.; Manzano, P.; Garcia, M. C.; Chicharro, J.; Puente, M.; Lorenzo, M.; Garcia, A.; Ferrer, S.; Gomez, R. M.; Fraile, M. T.; Lavandera, J. L.; Fiandor, J. M.; Vidal, J.; Herreros, E.; Gargallo-Viola, D. *Bioorg. Med. Chem. Lett.* **2013**, *23*, 6938.
(112) Winter, R. W.; Kelly, J. X.; Smilkstein, M. J.; Dodean, R.; Hinrichs, D.; Riscoe, M. K. *Exp. Parasitol.* **2008**, *118*, 487.
(113) Nilsen, A.; LaCrue, A. N.; White, K. L.; Forquer, I. P.; Cross, R. M.; Marfurt, J.; Mather, M. W.; Delves, M. J.; Shackleford, D. M.; Saenz, F. E.; Morrisey, J. M.; Steuten, J.; Mutka, T.; Li, Y.; Wirjanata, G.; Ryan, E.; Duffy, S.; Kelly, J. X.; Sebayang, B. F.; Zeeman, A. M.; Noviyanti, R.; Sinden, R. E.; Kocken, C. H.; Price, R. N.; Avery, V. M.; Angulo-Barturen, I.; Jimenez-Diaz, M. B.; Ferrer, S.; Herreros, E.; Sanz, L. M.; Gamo, F. J.; Bathurst, I.; Burrows, J. N.; Siegl, P.; Guy, R. K.; Winter, R. W.; Vaidya, A. B.; Charman, S. A.; Kyle, D. E.; Manetsch, R.; Riscoe, M. K. *Sci. Transl. Med.* **2013**, *5*, 177ra37.
(114) Smilkstein, M. J.; Forquer, I.; Kanazawa, A.; Kelly, J. X.; Winter, R. W.; Hinrichs, D. J.; Kramer, D. M.; Riscoe, M. K. *Mol. Biochem. Parasitol.* **2008**, *159*, 64.
(115) Jimenez-Diaz, M. B.; Mulet, T.; Viera, S.; Gomez, V.; Garuti, H.; Ibanez, J.; Alvarez-Doval, A.; Shultz, L. D.; Martinez, A.; Gargallo-Viola, D.; Angulo-Barturen, I. *Antimicrob. Agents Chemother.* **2009**, *53*, 4533.
(116) Dembele, L.; Gego, A.; Zeeman, A. M.; Franetich, J. F.; Silvie, O.; Rametti, A.; Le Grand, R.; Dereuddre-Bosquet, N.; Sauerwein, R.; van Gemert, G. J.; Vaillant, J. C.; Thomas, A. W.; Snounou, G.; Kocken, C. H.; Mazier, D. *PLoS One* **2011**, *6*, e18162.
(117) Hyde, J. E. *Curr. Drug Targets* **2007**, *8*, 31.
(118) Asahi, H.; Kanazawa, T.; Kajihara, Y.; Takahashi, K.; Takahashi, T. *Parasitology* **1996**, *113*, 19.
(119) Ting, L. M.; Shi, W.; Lewandowicz, A.; Singh, V.; Mwakingwe, A.; Birck, M. R.; Ringia, E. A.; Bench, G.; Madrid, D. C.; Tyler, P. C.; Evans, G. B.; Furneaux, R. H.; Schramm, V. L.; Kim, K. *J. Biol. Chem.* **2005**, *280*, 9547.
(120) (a) Berman, P. A.; Human, L. *Adv. Exp. Med. Biol.* **1991**, *309A*, 165. (b) Berman, P. A.; Human, L.; Freese, J. A. *J. Clin. Invest.* **1991**, *88*, 1848.
(121) (a) Madrid, D. C.; Ting, L. M.; Waller, K. L.; Schramm, V. L.; Kim, K. *J. Biol. Chem.* **2008**, *283*, 35899. (b) Ting, L. M.; Gissot, M.; Coppi, A.; Sinnis, P.; Kim, K. *Nat. Med.* **2008**, *14*, 954.
(122) Kline, P. C.; Schramm, V. L. *Biochemistry* **1993**, *32*, 13212.
(123) Erion, M. D.; Stoeckler, J. D.; Guida, W. C.; Walter, R. L.; Ealick, S. E. *Biochemistry* **1997**, *36*, 11735.
(124) Kline, P. C.; Schramm, V. L. *Biochemistry* **1992**, *31*, 5964.
(125) Miles, R. W.; Tyler, P. C.; Furneaux, R. H.; Bagdassarian, C. K.; Schramm, V. L. *Biochemistry* **1998**, *37*, 8615.
(126) Kicska, G. A.; Tyler, P. C.; Evans, G. B.; Furneaux, R. H.; Schramm, V. L.; Kim, K. *J. Biol. Chem.* **2002**, *277*, 3226.
(127) Kicska, G. A.; Tyler, P. C.; Evans, G. B.; Furneaux, R. H.; Kim, K.; Schramm, V. L. *J. Biol. Chem.* **2002**, *277*, 3219.
(128) Lewandowicz, A.; Tyler, P. C.; Evans, G. B.; Furneaux, R. H.; Schramm, V. L. *J. Biol. Chem.* **2003**, *278*, 31465.
(129) Taylor Ringia, E. A.; Schramm, V. L. *Curr. Top. Med. Chem.* **2005**, *5*, 1237.
(130) Lewandowicz, A.; Schramm, V. L. *Biochemistry* **2004**, *43*, 1458.
(131) Cassera, M. B.; Hazleton, K. Z.; Merino, E. F.; Obaldia, N., 3rd; Ho, M. C.; Murkin, A. S.; DePinto, R.; Gutierrez, J. A.; Almo, S. C.; Evans, G. B.; Babu, Y. S.; Schramm, V. L. *PLoS One* **2011**, *6*, e26916.
(132) Traut, T. W. *Mol. Cell. Biochem.* **1994**, *140*, 1.
(133) Baldwin, J.; Michnoff, C. H.; Malmquist, N. A.; White, J.; Roth, M. G.; Rathod, P. K.; Phillips, M. A. *J. Biol. Chem.* **2005**, *280*, 21847.
(134) Phillips, M. A.; Gujjar, R.; Malmquist, N. A.; White, J.; El Mazouni, F.; Baldwin, J.; Rathod, P. K. *J. Med. Chem.* **2008**, *51*, 3649.
(135) Gujjar, R.; Marwaha, A.; El Mazouni, F.; White, J.; White, K. L.; Creason, S.; Shackleford, D. M.; Baldwin, J.; Charman, W. N.;

Buckner, F. S.; Charman, S.; Rathod, P. K.; Phillips, M. A. *J. Med. Chem.* **2009**, *52*, 1864.
(136) Malmquist, N. A.; Gujjar, R.; Rathod, P. K.; Phillips, M. A. *Biochemistry* **2008**, *47*, 2466.
(137) (a) Topliss, J. G. *J. Med. Chem.* **1972**, *15*, 1006. (b) Topliss, J. G. *J. Med. Chem.* **1977**, *20*, 463.
(138) Deng, X.; Gujjar, R.; El Mazouni, F.; Kaminsky, W.; Malmquist, N. A.; Goldsmith, E. J.; Rathod, P. K.; Phillips, M. A. *J. Biol. Chem.* **2009**, *284*, 26999.
(139) Gujjar, R.; El Mazouni, F.; White, K. L.; White, J.; Creason, S.; Shackleford, D. M.; Deng, X.; Charman, W. N.; Bathurst, I.; Burrows, J.; Floyd, D. M.; Matthews, D.; Buckner, F. S.; Charman, S. A.; Phillips, M. A.; Rathod, P. K. *J. Med. Chem.* **2011**, *54*, 3935.
(140) Coteron, J. M.; Marco, M.; Esquivias, J.; Deng, X.; White, K. L.; White, J.; Koltun, M.; El Mazouni, F.; Kokkonda, S.; Katneni, K.; Bhamidipati, R.; Shackleford, D. M.; Angulo-Barturen, I.; Ferrer, S. B.; Jimenez-Diaz, M. B.; Gamo, F. J.; Goldsmith, E. J.; Charman, W. N.; Bathurst, I.; Floyd, D.; Matthews, D.; Burrows, J. N.; Rathod, P. K.; Charman, S. A.; Phillips, M. A. *J. Med. Chem.* **2011**, *54*, 5540.
(141) (a) Plouffe, D.; Brinker, A.; McNamara, C.; Henson, K.; Kato, N.; Kuhen, K.; Nagle, A.; Adrian, F.; Matzen, J. T.; Anderson, P.; Nam, T. G.; Gray, N. S.; Chatterjee, A.; Janes, J.; Yan, S. F.; Trager, R.; Caldwell, J. S.; Schultz, P. G.; Zhou, Y.; Winzeler, E. A. *Proc. Natl. Acad. Sci. U.S.A.* **2008**, *105*, 9059. (b) Smilkstein, M.; Sriwilaijaroen, N.; Kelly, J. X.; Wilairat, P.; Riscoe, M. *Antimicrob. Agents Chemother.* **2004**, *48*, 1803. (c) Bennett, T. N.; Paguio, M.; Gligorijevic, B.; Seudieu, C.; Kosar, A. D.; Davidson, E.; Roepe, P. D. *Antimicrob. Agents Chemother.* **2004**, *48*, 1807.
(142) Yeung, B. K.; Zou, B.; Rottmann, M.; Lakshminarayana, S. B.; Ang, S. H.; Leong, S. Y.; Tan, J.; Wong, J.; Keller-Maerki, S.; Fischli, C.; Goh, A.; Schmitt, E. K.; Krastel, P.; Francotte, E.; Kuhen, K.; Plouffe, D.; Henson, K.; Wagner, T.; Winzeler, E. A.; Petersen, F.; Brun, R.; Dartois, V.; Diagana, T. T.; Keller, T. H. *J. Med. Chem.* **2010**, *53*, 5155.
(143) Ames, B. N.; Lee, F. D.; Durston, W. E. *Proc. Natl. Acad. Sci. U.S.A.* **1973**, *70*, 782.
(144) Rottmann, M.; McNamara, C.; Yeung, B. K.; Lee, M. C.; Zou, B.; Russell, B.; Seitz, P.; Plouffe, D. M.; Dharia, N. V.; Tan, J.; Cohen, S. B.; Spencer, K. R.; Gonzalez-Paez, G. E.; Lakshminarayana, S. B.; Goh, A.; Suwanarusk, R.; Jegla, T.; Schmitt, E. K.; Beck, H. P.; Brun, R.; Nosten, F.; Renia, L.; Dartois, V.; Keller, T. H.; Fidock, D. A.; Winzeler, E. A.; Diagana, T. T. *Science* **2010**, *329*, 1175.
(145) Russell, B. M.; Udomsangpetch, R.; Rieckmann, K. H.; Kotecka, B. M.; Coleman, R. E.; Sattabongkot, J. *Antimicrob. Agents Chemother.* **2003**, *47*, 170.
(146) van Pelt-Koops, J. C.; Pett, H. E.; Graumans, W.; van der Vegte-Bolmer, M.; van Gemert, G. J.; Rottmann, M.; Yeung, B. K.; Diagana, T. T.; Sauerwein, R. W. *Antimicrob. Agents Chemother.* **2012**, *56*, 3544.
(147) (a) Leong, F. J.; Li, R.; Jain, J. P.; Lefevre, G.; Magnusson, B.; Diagana, T. T.; Pertel, P. *Antimicrob. Agents Chemother.* **2014**, *58*, 6209. (b) White, N. J.; Pukrittayakamee, S.; Phyo, A. P.; Rueangweerayut, R.; Nosten, F.; Jittamala, P.; Jeeyapant, A.; Jain, J. P.; Lefevre, G.; Li, R.; Magnusson, B.; Diagana, T. T.; Leong, F. J. *N. Engl. J. Med.* **2014**, *371*, 403.
(148) Dharia, N. V.; Sidhu, A. B.; Cassera, M. B.; Westenberger, S. J.; Bopp, S. E.; Eastman, R. T.; Plouffe, D.; Batalov, S.; Park, D. J.; Volkman, S. K.; Wirth, D. F.; Zhou, Y.; Fidock, D. A.; Winzeler, E. A. *Genome Biol.* **2009**, *10*, R21.
(149) (a) Trottein, F.; Thompson, J.; Cowman, A. F. *Gene* **1995**, *158*, 133. (b) Dyer, M.; Jackson, M.; McWhinney, C.; Zhao, G.; Mikkelsen, R. *Mol. Biochem. Parasitol.* **1996**, *78*, 1. (c) Krishna, S.; Woodrow, C.; Webb, R.; Penny, J.; Takeyasu, K.; Kimura, M.; East, J. M. *J. Biol. Chem.* **2001**, *276*, 10782.
(150) Kuhlbrandt, W. *Nat. Rev. Mol. Cell Biol.* **2004**, *5*, 282.
(151) Spillman, N. J.; Allen, R. J.; McNamara, C. W.; Yeung, B. K.; Winzeler, E. A.; Diagana, T. T.; Kirk, K. *Cell Host Microbe* **2013**, *13*, 227.
(152) Wu, T.; Nagle, A.; Kuhen, K.; Gagaring, K.; Borboa, R.; Francek, C.; Chen, Z.; Plouffe, D.; Goh, A.; Lakshminarayana, S. B.; Wu, J.; Ang, H. Q.; Zeng, P.; Kang, M. L.; Tan, W.; Tan, M.; Ye, N.; Lin, X.; Caldwell, C.; Ek, J.; Skolnik, S.; Liu, F.; Wang, J.; Chang, J.; Li, C.; Hollenbeck, T.; Tuntland, T.; Isbell, J.; Fischli, C.; Brun, R.; Rottmann, M.; Dartois, V.; Keller, T.; Diagana, T.; Winzeler, E.; Glynne, R.; Tully, D. C.; Chatterjee, A. K. *J. Med. Chem.* **2011**, *54*, 5116.
(153) Liu, B.; Chang, J.; Gordon, W. P.; Isbell, J.; Zhou, Y.; Tuntland, T. *Drug Discovery Today* **2008**, *13*, 360.
(154) Meister, S.; Plouffe, D. M.; Kuhen, K. L.; Bonamy, G. M.; Wu, T.; Barnes, S. W.; Bopp, S. E.; Borboa, R.; Bright, A. T.; Che, J.; Cohen, S.; Dharia, N. V.; Gagaring, K.; Gettayacamin, M.; Gordon, P.; Groessl, T.; Kato, N.; Lee, M. C.; McNamara, C. W.; Fidock, D. A.; Nagle, A.; Nam, T. G.; Richmond, W.; Roland, J.; Rottmann, M.; Zhou, B.; Froissard, P.; Glynne, R. J.; Mazier, D.; Sattabongkot, J.; Schultz, P. G.; Tuntland, T.; Walker, J. R.; Zhou, Y.; Chatterjee, A.; Diagana, T. T.; Winzeler, E. A. *Science* **2011**, *334*, 1372.
(155) Nagle, A.; Wu, T.; Kuhen, K.; Gagaring, K.; Borboa, R.; Francek, C.; Chen, Z.; Plouffe, D.; Lin, X.; Caldwell, C.; Ek, J.; Skolnik, S.; Liu, F.; Wang, J.; Chang, J.; Li, C.; Liu, B.; Hollenbeck, T.; Tuntland, T.; Isbell, J.; Chuan, T.; Alper, P. B.; Fischli, C.; Brun, R.; Lakshminarayana, S. B.; Rottmann, M.; Diagana, T. T.; Winzeler, E. A.; Glynne, R.; Tully, D. C.; Chatterjee, A. K. *J. Med. Chem.* **2012**, *55*, 4244.
(156) Harris, C. J.; Hill, R. D.; Sheppard, D. W.; Slater, M. J.; Stouten, P. F. *Comb. Chem. High Throughput Screening* **2011**, *14*, 521.
(157) Younis, Y.; Douelle, F.; Feng, T. S.; Gonzalez Cabrera, D.; Le Manach, C.; Nchinda, A. T.; Duffy, S.; White, K. L.; Shackleford, D. M.; Morizzi, J.; Mannila, J.; Katneni, K.; Bhamidipati, R.; Zabiulla, K. M.; Joseph, J. T.; Bashyam, S.; Waterson, D.; Witty, M. J.; Hardick, D.; Wittlin, S.; Avery, V.; Charman, S. A.; Chibale, K. *J. Med. Chem.* **2012**, *55*, 3479.
(158) Gamo, F. J.; Sanz, L. M.; Vidal, J.; de Cozar, C.; Alvarez, E.; Lavandera, J. L.; Vanderwall, D. E.; Green, D. V.; Kumar, V.; Hasan, S.; Brown, J. R.; Peishoff, C. E.; Cardon, L. R.; Garcia-Bustos, J. F. *Nature* **2010**, *465*, 305.
(159) Lombardo, F.; Shalaeva, M. Y.; Tupper, K. A.; Gao, F. *J. Med. Chem.* **2001**, *44*, 2490.
(160) Bevan, C. D.; Lloyd, R. S. *Anal. Chem.* **2000**, *72*, 1781.
(161) Valko, K.; Nunhuck, S.; Bevan, C.; Abraham, M. H.; Reynolds, D. P. *J. Pharm. Sci.* **2003**, *92*, 2236.
(162) Gonzalez Cabrera, D.; Douelle, F.; Younis, Y.; Feng, T. S.; Le Manach, C.; Nchinda, A. T.; Street, L. J.; Scheurer, C.; Kamber, J.; White, K. L.; Montagnat, O. D.; Ryan, E.; Katneni, K.; Zabiulla, K. M.; Joseph, J. T.; Bashyam, S.; Waterson, D.; Witty, M. J.; Charman, S. A.; Wittlin, S.; Chibale, K. *J. Med. Chem.* **2012**, *55*, 11022.
(163) Younis, Y.; Douelle, F.; Gonzalez Cabrera, D.; Le Manach, C.; Nchinda, A. T.; Paquet, T.; Street, L. J.; White, K. L.; Zabiulla, K. M.; Joseph, J. T.; Bashyam, S.; Waterson, D.; Witty, M. J.; Wittlin, S.; Charman, S. A.; Chibale, K. *J. Med. Chem.* **2013**, *56*, 8860.